Atmos. Chem. Phys., 7, 2987–3013, 2007
www.atmos-chem-phys.net/7/2987/2007/

Atmospheric Chemistry and Physics

Lightning-produced NO_x over Brazil during TROCCINOX: airborne measurements in tropical and subtropical thunderstorms and the importance of mesoscale convective systems

H. Huntrieser[1], H. Schlager[1], A. Roiger[1], M. Lichtenstern[1], U. Schumann[1], C. Kurz[1], D. Brunner[2,*], C. Schwierz[2], A. Richter[3], and A. Stohl[4]

[1]Institut für Physik der Atmosphäre, Deutsches Zentrum für Luft- und Raumfahrt (DLR), Oberpfaffenhofen, Weßling, Germany
[2]Institute for Atmospheric and Climate Science, ETH Zurich, Switzerland
[3]Institute of Environmental Physics (IUP), University of Bremen, Germany
[4]Norwegian Institute for Air Research (NILU), Dept. Regional and Global Pollution Issues, Kjeller, Norway
[*]now at: Laboratory for Air Pollution and Environmental Technology, Empa, Swiss Federal Laboratories for Materials Testing and Research, Dübendorf, Switzerland

Received: 30 January 2007 – Published in Atmos. Chem. Phys. Discuss.: 22 February 2007
Revised: 25 May 2007 – Accepted: 25 May 2007 – Published: 12 June 2007

Abstract. During the TROCCINOX field experiments in February–March 2004 and February 2005, airborne in situ measurements of NO, NO_y, CO, and O_3 mixing ratios and the $J(NO_2)$ photolysis rate were carried out in the anvil outflow of thunderstorms over southern Brazil. Both tropical and subtropical thunderstorms were investigated, depending on the location of the South Atlantic convergence zone. Tropical air masses were discriminated from subtropical ones according to the higher equivalent potential temperature (Θ_e) in the lower and mid troposphere, the higher CO mixing ratio in the mid troposphere, and the lower wind velocity in the upper troposphere within the Bolivian High (north of the subtropical jet stream). During thunderstorm anvil penetrations, typically at 20–40 km horizontal scales, NO_x mixing ratios were distinctly enhanced and the absolute mixing ratios varied between 0.2–1.6 nmol mol^{-1} on average. This enhancement was mainly attributed to NO_x production by lightning and partly due to upward transport from the NO_x-richer boundary layer. In addition, CO mixing ratios were occasionally enhanced, indicating upward transport from the boundary layer. For the first time, the composition of the anvil outflow from a large, long-lived mesoscale convective system (MCS) advected from northern Argentina and Uruguay was investigated in more detail. Over a horizontal scale of about 400 km, NO_x, CO and O_3 absolute mixing ratios were significantly enhanced in these air masses in the range of 0.6–1.1, 110–140 and 60–70 nmol mol^{-1}, respectively. Analyses from trace gas correlations and a Lagrangian particle dispersion model indicate that polluted air masses, probably from the Buenos Aires urban area and from biomass burning regions, were uplifted by the MCS. Ozone was distinctly enhanced in the aged MCS outflow, due to photochemical production and entrainment of O_3-rich air masses from the upper troposphere – lower stratosphere region. The aged MCS outflow was transported to the north, ascended and circulated, driven by the Bolivian High over the Amazon basin. In the observed case, the O_3-rich MCS outflow remained over the continent and did not contribute to the South Atlantic ozone maximum.

Correspondence to: H. Huntrieser
(heidi.huntrieser@dlr.de)

1 Introduction

Knowledge of the lightning-induced nitrogen oxides (LNO_x) source is important for understanding and predicting the nitrogen oxides (NO_x=NO+NO_2) concentration and photochemical ozone (O_3) formation in the troposphere (Crutzen, 1970; Chameides and Walker, 1973), among others. NO_x in the presence of oxidised products (RO_x) from NMHC, CO or CH_4, acts as a catalyst for the production of O_3, which is a major greenhouse gas in the upper troposphere.

The amount of nitrogen mass induced by lightning annually and globally is still very uncertain. In spite of more than four decades of research on this topic, reviewed in detail in Schumann and Huntrieser (2007), typical estimates range from 1 to 14 Tg yr^{-1}, with some clustering of the estimates near 5 Tg yr^{-1}, see, e.g., Huntrieser et al. (1998, 2002) and

Beirle et al. (2006). LNO_x has a disproportional large influence on tropospheric chemistry, since the lifetime of NO_x is much longer in the upper troposphere (UT) (2–5 days) than in the boundary layer (BL) (<1 day) (Jacob et al., 1996; Schultz et al., 1999). Moreover, the photochemistry in the free troposphere is mostly NO_x limited (Jaeglé et al., 1999). Hence, the ozone production potential is higher in the UT than in the BL (Strand and Hov, 1996).

In the past, several dedicated LNO_x field experiments have been performed in Europe and the United States, mainly at midlatitudes (e.g. LINOX, EULINOX and STERAO) (Luke et al., 1992; Ridley et al., 1994; Poulida et al., 1996; Ridley et al., 1996; Huntrieser et al., 1998; Höller et al., 1999; Stith et al., 1999; Dye et al., 2000; Huntrieser et al., 2002) and partly in the subtropics (e.g. CRYSTAL-FACE) (Ridley et al., 2004), see also overview in Schumann and Huntrieser (2007). However, more than 75% of all lightning flashes occur in the tropics and subtropics between 35° S and 35° N, mainly over the continents (Christian et al., 1999; Bond et al., 2002; Christian et al., 2003). It has been suggested that the total source strengths of the main UT- and BL-NO_x sources in this region, lightning and biomass burning, are comparable (Smyth et al., 1996). The variability of the tropospheric ozone column is dominated by these two sources (Martin et al., 2000). However, even for 5 Tg yr^{-1} of LNO_x production, LNO_x is the dominant NO_x source in the UT in the tropics and about 30% of tropospheric O_3 is formed by enhanced photochemistry due to LNO_x (Lamarque et al., 1996; Smyth et al., 1996; Levy et al., 1996; 1999; Grewe et al., 2001; Hauglustaine et al., 2001; Sauvage et al., 2007). Therefore, measurements in the tropics are needed to assess the production of LNO_x more accurately.

So far, rather few measurements have been performed near tropical thunderstorms over the South American continent. In 1982, on a flight from Frankfurt (Germany) to São Paulo (Brazil), enhanced NO_x mixing ratios (~0.4 nmol mol^{-1} or ppbv) were for the first time encountered along the eastern coast of Brazil, which were partly attributed to production by lightning (Dickerson, 1984). A few years later, during the GTE/ABLE 2A mission over the Amazon basin in 1985, mixing ratios up to 0.2 nmol mol^{-1} NO were observed in regions of electrically active clouds (Torres and Buchan, 1988). During the GTE/TRACE-A experiment in September–October 1992 in Brazil (end of dry season) upper tropospheric NO plumes, that covered horizontal spatial scales between 100 and 1000 km, were observed (Pickering et al., 1996; Smyth et al., 1996). NO mixing ratios up to 1.3 nmol mol^{-1} were found in these plumes that originated from deep convection (MCS), containing NO emissions from both biomass burning and lightning. On a transfer flight from Panama to Santiago de Chile during the INCA experiment in March–April 2000, elevated NO and NO_y mixing ratios (0.8 and 1.8 nmol mol^{-1}) were observed between 4° S and 8° S downwind of Brazilian thunderstorms active 8 h before (Baehr et al., 2003).

Here we present measurements from the "Tropical Convection, Cirrus, and Nitrogen Oxides Experiment" (TROCCINOX) over the State of São Paulo and surroundings in Brazil (10° S to 28° S and 38° W to 55° W). This tropical-subtropical lightning-rich region was selected since we wanted to compare our previous observations in midlatitude thunderstorms (Huntrieser et al., 1998, 2002) with measurements in other regions. Two field experimental phases were carried out in February–March 2004 and in February 2005 (see Sects. 2 and 3). For the first time, detailed airborne measurements were performed in the anvil outflow of Brazilian thunderstorms in the wet season. We mainly analyse meteorological and trace gas measurements carried out with the DLR (Deutsches Zentrum für Luft- und Raumfahrt) Falcon research aircraft in the outflow of tropical and subtropical thunderstorms (see Sects. 3, 4 and 5). The meteorological environment in which the thunderstorms developed is described in detail and the distinction between tropical and subtropical environments is defined (Sects. 3–4). We further focus our observations on an aged anvil outflow from a large, long-lived MCS system over northern Argentina and Uruguay, since observations in the vicinity of South American MCS are rare in comparison to MCS occurring over North America (see Sects. 3 and 5). The results are discussed and summarized in Sect. 6. In a forthcoming paper, the selected airborne measurements presented here will be combined with lightning and radar observations to quantify the amount of LNO_x produced by the different thunderstorm types (Huntrieser et al., 2007[1]). Results obtained with two further aircraft are to be reported elsewhere.

2 Data and model description

2.1 Airborne instrumentation: Falcon

The airborne measurements up to 12.5 km altitude were carried out with the DLR Falcon aircraft, which was equipped with DLR instruments to measure NO, NO_y, O_3, and CO mixing ratios and the photolysis rate $J(NO_2)$. The instrumentation has been used during several field campaigns in the past (Table 1). All instruments are capable of measuring at high temporal resolution (1–5 s), as necessary for investigating the small scale structures in the anvil outflow (Huntrieser et al., 1998; Höller et al., 1999; Huntrieser et al., 2002). The NO_2 (and NO_x) mixing ratios are calculated from the photostationary steady state equation from the measurements of NO, O_3, $J(NO_2)$, pressure and temperature. Since O_3 is not available during the anvil penetrations for reasons explained below, ambient O_3 mixing ratios outside the anvils are used instead.

In addition, position, altitude, temperature, humidity, pressure, and the 3-dimensional wind vector (u,v,w) were measured with the standard Falcon meteorological measurement

[1] Huntrieser, H. et al., in preparation, 2007.

Table 1. Selected Falcon instrumentation.

Species	Technique	Averaging Time, s	Accuracy, %	Precision, %	Reference
NO	chemiluminescence	1	10	3	Schlager et al. (1997), Baehr et al. (2003)
NO_y	chemiluminescence plus Au-converter	1	15	5	Schlager et al. (1997), Baehr et al. (2003) Huntrieser et al. (2005)
O_3	UV absorption	5	5	1	Baehr et al. (2003), Huntrieser et al. (2005)
CO	VUV fluorescence	1	10	3	Gerbig et al. (1999), Baehr et al. (2003), Huntrieser et al. (2005)
$J(NO_2)$	filter radiometer	1	6	0.0001, s^{-1}	Volz-Thomas et al. (1996), Huntrieser et al. (2002)

system (Schumann et al., 1995). The outside air temperature is measured by an open wire PT100 sensor mounted in a Rosemount Type 102 total air temperature housing. The humidity data represent a composite derived from three different sensors (a dewpoint mirror, a capacitive sensor and a Lyman Alpha absorption instrument). All flight altitude values refer to pressure height and UTC (Universal Time Coordinated) time. The time difference between UTC and the Brazilian (Summer) Time (BR(S)T) in the TROCCINOX observation area is 2 h in the austral summer (until 14 February 2004 and 19 February 2005) and 3 h in the austral winter (e.g. 16 BRST=18:00 UTC and 15 BRT=18:00 UTC).

During several anvil penetrations, strongly enhanced O_3 signals in the range ($\sim$100–300 nmol mol^{-1}) were measured. In Sect. 3.3.1 measurements from such a flight on 28 February 2004 are shown as an example and discussed in detail. Influence by entrainment of O_3-rich air from the tropopause region or lower stratosphere was excluded as explanation for the O_3 enhancement, since CO was also enhanced in most of the anvils. Furthermore, the O_3 mixing ratios are too high to be explained by photochemical production or by vertical transport from the BL, where in general lower mixing ratios between $\sim$20–50 nmol mol^{-1} were measured. These pronounced O_3 enhancements were always connected to penetrations in the anvil outflow and never outside. From the discussion of the flight in Sect. 3.3.1 we consider the high O_3 signals to be artefacts and excluded such elevated signals from the data set. Similar ozone-rich transients have been observed during CARIBIC and MOZAIC flights performed mainly during in-cloud sections in the tropics (Zahn et al., 2002). Recently, Ridley et al. (2006) discussed several possible reasons for observed spikes in O_3 (and NO) signals during CRYSTAL-FACE and other airborne field experiments. They suggested that the observed short-term spikes ($\sim$1 s) during CRYSTAL-FACE were measurement artefacts caused by discharges on the aircraft fuselage or inlets. However, during TROCCINOX the artefact O_3 signals were much broader and covered the entire duration of the anvil penetration ($\sim$20–40 km, $\sim$several minutes). In addition, measurements during the TROCCINOX field campaign in 2005 with an additional O_3 instrument (with different inlet design) indicate that discharges on inlets were probably not the reason for the artefact O_3 signals. Meyer et al. (1991) have reported on a water vapour interference for ground-based measurements of O_3 for some of the instruments using the UV absorption technique (same technique as used on the Falcon) which may explain our observations. The interference can be significant when the humidity is varying rapidly as during anvil penetrations. The reason for the interference, as suggested by Meyer et al., could be humidity-induced variations of the extinction of UV light by the windows of the two optical cells in the instrument. First tests in the laboratory with the Falcon O_3 instrument indicate an interference due to abrupt changing water vapour mixing ratios in accordance with Meyer et al. (1991). However, further laboratory studies are needed to study the interference in more detail and the results will be reported in a separate paper.

2.2 LNO_x forecasts: ECHAM5/MESSy

For flight planning during the TROCCINOX field phases, a variety of model forecasts based on data from the European Centre for Medium-Range Weather Forecasts (ECMWF) were used. In addition, forecasts of the horizontal LNO_x distribution over South America were provided using the coupled atmospheric chemistry global circulation model (GCM) ECHAM5/MESSy (preliminary version 0.9, further denoted as E5M0) (Kurz, 2006). The model uses the latest version 5 of the ECHAM GCM (ECMWF model, Hamburg version) (Roeckner et al., 2006) together with a chemical submodel MECCA (Module Efficiently Calculating the Chemistry of the Atmosphere) (Sander et al., 2005). Both are coupled using the Modular Earth Submodel System (MESSy) (Jöckel et al., 2005, 2006). The Tiedke mass flux scheme for deep, mid-level and shallow convection is implemented. The model was run in a spectral T63 resolution and 19 layers in the vertical, with the uppermost model layer centred at 10 hPa. The model time step is 20 min. A nudging technique (see e.g. Jeuken et al., 1998) was applied to relax the models

prognostic variables (divergence, vorticity, temperature, and surface pressure) towards operational ECMWF model forecasts (available every 6 h). E-folding relaxation times of 12 h for temperature and surface pressure, 6 h for vorticity, and 48 h for divergence were used. The chemical mechanism comprises 104 gas phase species, including non-methane hydrocarbons and 245 reactions, and heterogeneous reactions on polar stratospheric cloud particles. Lightning flash rates and the resulting lightning NO emissions are parameterized according to Grewe et al. (2001), relating the flash frequency to the vertical mass flux within a convective clouds updrafts. The ratio of intra-cloud and cloud-to-ground flashes is calculated following Price and Rind (1993). The NO emission per flash is scaled to result in a mean annual global emission of 5 Tg(N). In the vertical, a "C-shape" fit, conserving the shape of the profiles derived by Pickering et al. (1998), is used to distribute the emitted lightning NO.

2.3 Transport modelling: FLEXPART

The transport of air masses was simulated with the Lagrangian particle dispersion model FLEXPART (see http://zardoz.nilu.no/~andreas/flextra+flexpart.html) (Stohl et al., 1998, 2005). In the past, the model has mainly been used for studying long-range air pollution transport from North America to Europe (e.g. Stohl et al., 2003; Huntrieser et al., 2005).

FLEXPART was run backward in time from small segments along the flight tracks. The backward simulation method, described in more detail by Stohl et al. (2003) and Seibert and Frank (2004), can be used to analyse transport pathways of air masses from potential source regions to each of the Falcon flight segments. Whenever the aircraft changes its position by more than 0.2° or its altitude by 50 m below 300 m, 150 m below 1000 m, 200 m below 3000 m, or 400 m above 3000 m, a backward simulation is initiated. Each simulation consists of 40 000 particles released in the volume of air sampled and followed 20 days backward in time. A potential emission sensitivity function is calculated which is proportional to the residence times of the particles in a particular 3-D grid cell. Its value is a measure for the simulated mixing ratio at the receptor that a source of unit strength in the respective grid cell would produce, disregarding loss processes.

All FLEXPART simulations presented here are based on global operational data from ECMWF with a horizontal resolution of 1°, 60 vertical levels and a time resolution of 3 h (analyses at 00:00, 06:00, 12:00, 18:00 UTC; 3-h forecasts at 03:00, 09:00, 15:00, 21:00 UTC). Wind fields with 0.5° resolution, covering the domain 90° W to 20° E and 40° S to 20° N, were nested into the global data in order to achieve higher resolution over the region of main interest. FLEXPART treats advection and turbulent diffusion by calculating the trajectories of a multitude of particles. Stochastic fluctuations, obtained by solving Langevin equations, are superimposed on the grid-scale winds to represent transport by turbulent eddies, which are not resolved in the ECMWF data. To account for sub-gridscale moist convective transport, the convection scheme by Emanuel and Živcovizc'-Rothman (1999) was implemented and tested by Forster et al. (2007).

3 Field experiment and observations in anvils

3.1 General trace gas, thunderstorm and lightning conditions over Brazil

The TROCCINOX operation area, in the SW-SE part of Brazil, is located within the range of the South Atlantic convergence zone (SACZ), an important climatological feature of the austral summer (Kodama, 1992; 1993; Satyamurty et al., 1998; Carvalho et al., 2002, 2004). The SACZ is a convective frontal zone originating in the Amazon basin and extending to southeastern Brazil and the subtropical Atlantic Ocean, which, however, may exhibit large variability in its geographical extension. The SACZ separates tropical and subtropical air masses originating over the Amazon basin and the Pacific Ocean, respectively (see Sect. 3.3.4). The formation of thunderstorms over Brazil depends on local conditions (e.g. orographic initiation), the presence of frontal zones such as the SACZ and the position of the Bolivian High (Pinto and Pinto, 2003; Siqueira et al., 2005). The convective systems occur on a wide range of temporal and spatial scales.

The anvil outflow from Brazilian thunderstorms may be redistributed over large areas (mainly between the equator and 20–30° S) as it circulates around the Bolivian High, a persistent upper level anticyclonic flow over tropical South America (Jonquieres and Marenco, 1998). In the vicinity of the Bolivian High, enhanced CO and NO_y mixing ratios have been observed over extended areas in the UT during several TROPOZ II and INCA flights (Jonquieres and Marenco, 1998; Baehr et al., 2003). In the wet season, the enhancement in NO_y is mainly attributed to production by lightning. Biogenic emissions from the rain forest in the Amazon basin are the main sources of CO (80–110 nmol mol^{-1}), which are transported upward by deep convection (Jonquieres and Marenco, 1998; Gatti et al., 2001). CO is produced by photochemical oxidation of isoprene emitted from vegetation (Harriss et al., 1990) and by direct emissions from the forest (Jacob and Wofsy, 1990). In contrast, O_3 and NO mixing ratios are low in the BL in the wet season with ~20 and ~0.05 nmol mol^{-1}, respectively (Jonquieres and Marenco, 1998). The Amazon rain forest is an efficient sink for O_3 and soil emissions rates of NO are low (Jacob and Wofsy, 1990).

Depending on season, large mesoscale convective systems (MCS; Houze, 1993, 2004) and mesoscale convective complexes (MCC; Maddox, 1980) occur rather frequently (maximum in January) in the SW part of Brazil (see global

distribution of MCS and MCC in Houze, 2004, Fig. 4, and Laing and Fritsch, 1997, Fig. 3). These systems typically move from northern Argentina and Paraguay to SW Brazil (Velasco and Fritsch, 1987). The MCS originate in the foothills of the Andes Mountains when warm and moist air masses from the Amazon basin are advected southward with the South American low-level jet to the central plains of southeastern South America (Laing and Fritsch, 1997; Nesbitt et al., 2000; Salio et al., 2007). Only sparse information on MCS over South America is available (Machado et al., 1998; Satyamurty et al., 1998; Salio et al., 2007), but their severity is at least similar to MCS over the central United States (Brooks et al., 2003). In these South American MCS, the highest flash rates globally occur (>1300 flashes per minute), as observed from space by the Lightning Imaging Sensor (LIS) (Cecil et al., 2005). In the subtropical Americas, the worldwide greatest spatial density of storms with very high flash rates occurs (Zipser et al., 2006) and this regions may be one of the most active areas for sprite production globally (Sato and Fukunishi, 2003; Thomas et al., 2007). Furthermore, these intense storms are characterised by extreme heights of the 40 DBz radar reflectivity contour between 16.75 and 19.5 km (Zipser et al., 2006).

Brazil is a country with a high lightning activity (50–70 millions CG flashes per year) and a high flash density (up to 10–15 flashes $km^{-2}\,yr^{-1}$) comparable to Florida (Pinto and Pinto, 2003). The majority of CG flashes over Brazil are negative flashes (Saba et al., 2006). Depending on different wind regimes, varying lightning activity has been observed over the Amazon region. During easterly (dryer) wind regimes at 850–700 hPa, more CG lightning activity within deeper and more intense thunderstorms were found than during westerly (more humid) wind regimes (Carvalho et al., 2002; Petersen et al., 2002).

3.2 Brief experimental overview

An overview on the project and the flights performed within TROCCINOX, see http://www.pa.op.dlr.de/troccinox/, will be given in a forthcoming paper (Schumann et al., 2007[2]). In 2004, the flights were carried out from Gaviao Peixoto (21.8° S, 48.4° W, ~560 m a.s.l.). In 2005, the operation base was in Aracatuba (21.1° S, 50.4° W, ~360 m a.s.l.). Most of the flights in southern Brazil (10° S to 28° S and 38° W to 55° W) were performed in subtropical air masses south of the SACZ. A few flights were performed in tropical air masses within the SACZ, e.g. 4–5 February 2005.

For classification of the thunderstorm environment as tropical or subtropical, a combination of equivalent potential temperature (Θ_e) and wind is used as summarized below (illustrated in more detail in Sects. 3 and 4). The Θ_e temperature is a suitable "tracer" of air masses, since it is conserved for both dry and moist adiabatic processes during transport. Tropical air masses are warm and humid, and therefore characterised by higher Θ_e values. Thunderstorms were only defined as "tropical" when the following criteria were fulfilled simultaneously for an air mass: 1) SACZ located over or to the south of the observation area, 2) $\Theta_e \geq 345$ K at 850 hPa and ≥ 332 K at 500 hPa, 3) circulation within the Bolivian High connected (in general) to low wind velocities in the UT (north of the subtropical jet stream). In addition, FLEXPART backward simulations were used (not shown in detail) to trace back the air masses to confirm the tropical (circulation within the Bolivian High) or subtropical (Pacific) air mass origin (see also FLEXPART example in Sect. 3.3.4 and http://zardoz.nilu.no/~andreas/TROCCINOX/). However, for thunderstorms located close to the SACZ the clear air mass determination was sometimes difficult. The criteria presented here for the separation of tropical and subtropical air masses are only valid for the investigated TROCCINOX area and period.

For the computation of Θ_e for a water-saturation pseudo-adiabatic process, the formula developed by Bolton (1980) was used for Falcon and ECMWF data:

$$\Theta_e = T_K \left(\frac{1000}{p}\right)^{0.2854(1-0.28\times10^{-3}r)} \times \exp\left[\left(\frac{3.376}{T_L} - 0.00254\right) \times r\,(1 + 0.81 \times 10^{-3} r)\right] \quad (1)$$

where r is the mixing ratio of water vapour ($g\,kg^{-1}$), T_K is the absolute temperature (K), p is the pressure (hPa) and T_L is the temperature at the lifting condensation level (K):

$$T_L = \frac{1}{\frac{1}{T_K - 55} - \frac{\ln(U/100)}{2840}} + 55 \quad (2)$$

where U is the relative humidity (%).

The general trace gas situation during the TROCCINOX flights is shown in Figs. 1a–c. NO_x, CO and O_3 data from all local TROCCINOX flights in 2004 and 2005 (25 flights, except the flight on 5 February 2005 for which no NO_x data are available) have been averaged over 250 m altitude bins (plotted in different colours). The mean profiles from these single flights were averaged once more and the result (overall mean) is shown in white. Generally, the vertical CO and NO_x profiles indicate a rather clean BL (<2 km) over the TROCCINOX area (NO_x: 0.10–0.25, CO: 90–110 nmol mol^{-1}), since it is located more than 500 km away from larger cities like São Paulo. Only during one period, 3–4 March 2004, the BL was more polluted (mean NO_x 0.3–0.5 and CO 110–160 nmol mol^{-1}), which may have been caused by vegetation fires in Paraguay and Uruguay at that time (see Sect. 3.3.2). Between 8 and 12 km altitude, NO_x mixing ratios are enhanced in the anvil outflow region, but on average stay below 1 nmol mol^{-1}. The flat C-shape of the CO profile and the broad range of mixing ratios in the free troposphere (40–130 nmol mol^{-1}) will be discussed in more detail in Sect. 3.3.4. Minimum CO mixing ratios of 40 to

[2]Schumann, U. et al., in preparation, 2007.

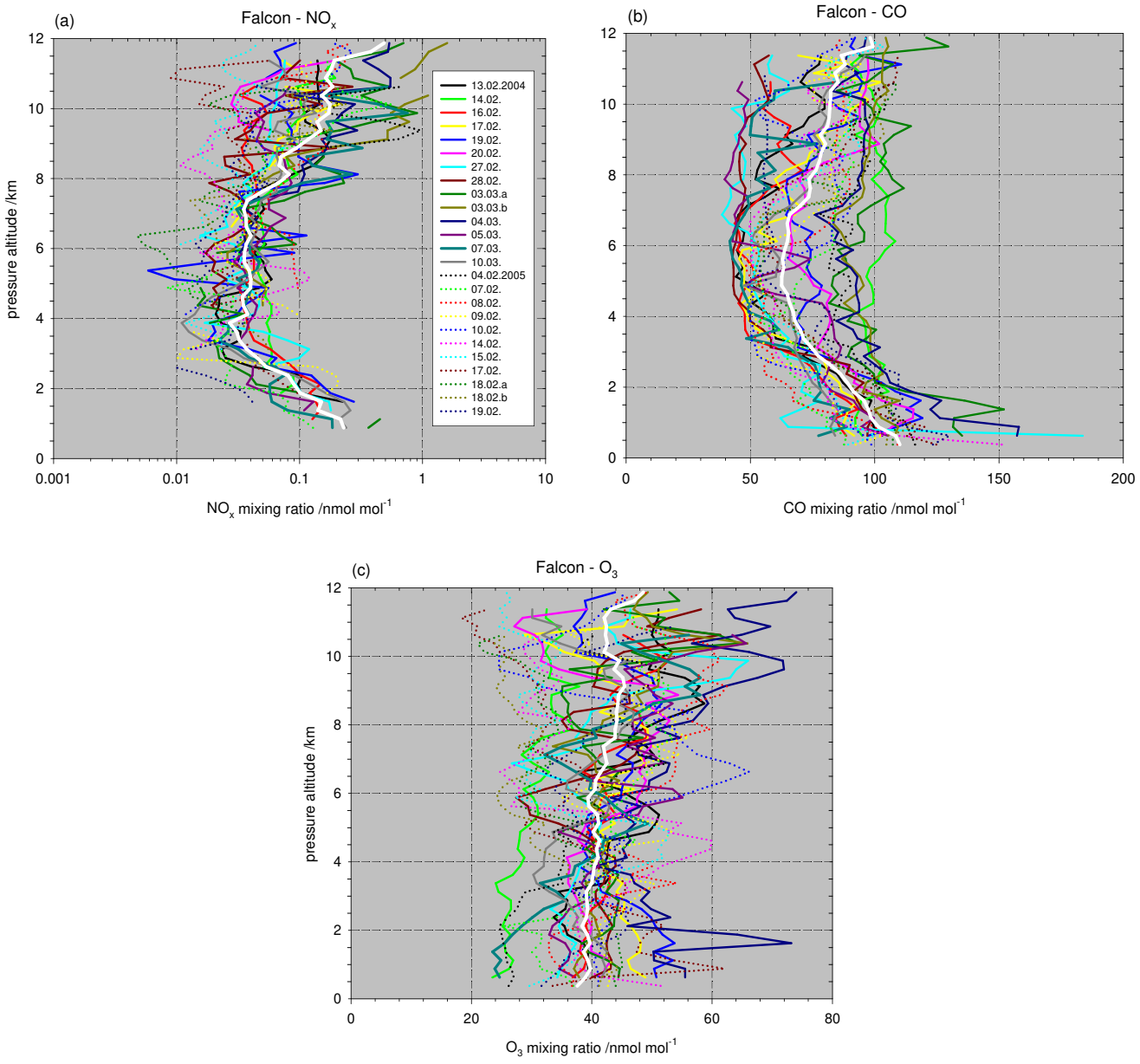

Fig. 1. Mean vertical NO_x **(a)**, CO **(b)** and O_3 **(c)** profiles derived from measurements with the Falcon aircraft (artificial O_3 measurements in clouds excluded). Mean values for every 250 m altitude bin are given for all TROCCINOX flights (dd:mm:yyyy) in colour, except for the flight on 5 February 2005 (no NO_x data available). The white lines are the mean of all coloured flight profiles in each figure.

60 nmol mol^{-1} are found in the mid troposphere between 4 and 7 km, except in tropical air masses (3–4 March 2004 and 4 February 2005) where CO is elevated (>70 nmol mol^{-1}) and almost constant throughout the free troposphere, indicating efficient vertical mixing. The overall O_3 mean profile indicates slightly increasing mixing ratios with height, on average from 40 to 50 nmol mol^{-1}.

3.3 Airborne measurements in anvils

In the next four subsections, measurements in the anvil outflow region during four TROCCINOX flights on 28 February and 7 March 2004, and on 4 and 18 February 2005 are presented. Some of these and further TROCCINOX flights with anvil penetrations have been described by Schumann et al. (2004) in brief, by Mari et al. (2006) who report on model simulations with Meso-NH for the 3–4 March 2004 flights, and by Chaboureau et al. (2007) who present simulations

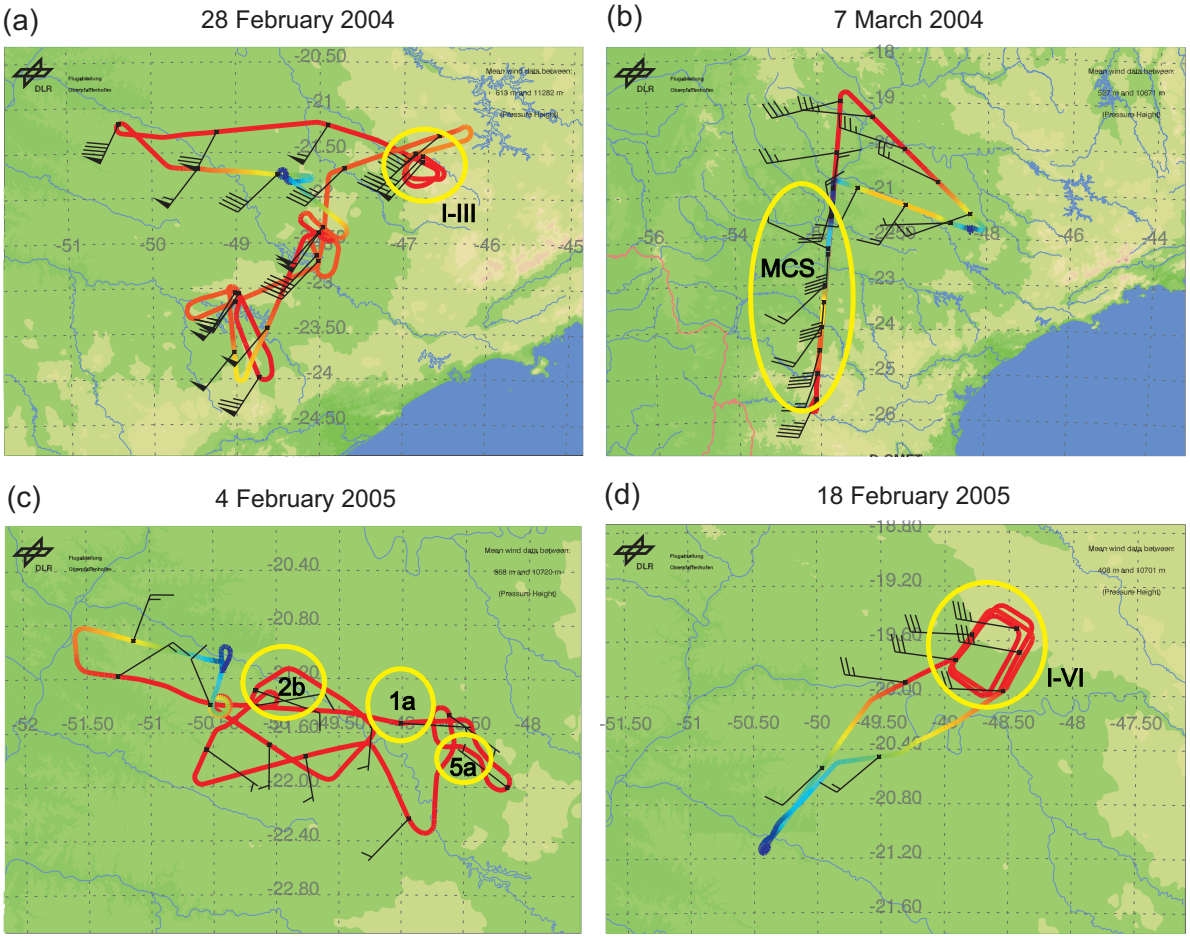

Fig. 2. Falcon flight tracks on **(a)** 28 February 2004 at 17:08–20:47 UTC, **(b)** 7 March 2004 at 11:53–15:24 UTC, **(c)** 4 February 2005 at 17:46–20:11 UTC, and **(d)** 18 February 2005 at 20:09–21:49 UTC with pressure height (coloured from blue to red with increasing height), wind direction (vane) and velocity (in knots, short 5, long 10, triangle 50). The areas with anvil penetrations are marked with circles and labelled (see also Fig. 6). The size of the domain in E–W and N–S direction is in **(a)** ~450×300 km^2, **(b)** ~1200×750 km^2, **(c)** ~400×250 km^2, and **(d)** ~450×300 km^2.

with a cloud resolving model for the 4 February 2005 case. The four selected flights mentioned above were found to be representative for the different thunderstorm types occurring during the field experiments. Furthermore, these flights featured a large number of anvil penetrations and exhibited pronounced signals in the trace gas mixing ratios. In addition to nitrogen oxides, measurements of CO and O_3 are discussed since they reflect the transport of polluted air masses from the BL into the anvil region and the downwind photochemistry. The importance of MCS as a major source of elevated NO_x and O_3 in the UT over the TROCCINOX area is illustrated in a case study. In addition, the specific thermodynamic and chemical characteristics of thunderstorms originating in subtropical and tropical air masses are highlighted in this section and will be discussed in further detail together with lightning and radar data in a forthcoming paper (Huntrieser et al., 2007[1]).

In the next four subsections, the four selected flights are described in more detail from a set of figures (a–d). To avoid repetition in every subsection and too many cross references, these figures (Figs. 2–5) are in general not mentioned specifically. The figure contents are briefly mentioned here. In Fig. 2 Falcon flight tracks and Falcon wind velocity and direction are presented. The positions of the investigated thunderstorms relative to the flight track are highlighted. In Fig. 3 GOES IR-images of clouds are shown together with the Falcon flight track and the position of the SACZ (roughly indicated along the leading line of the frontal cloud zone). In Fig. 4 and Fig. 5 horizontal distributions of the Θ_e temperature and wind at 850 hPa, and stream lines and the wind velocity at 200 hPa, respectively, based on ECMWF analyses are presented, which also indicate the position of the SACZ, the subtropical jet and the Bolivian High.

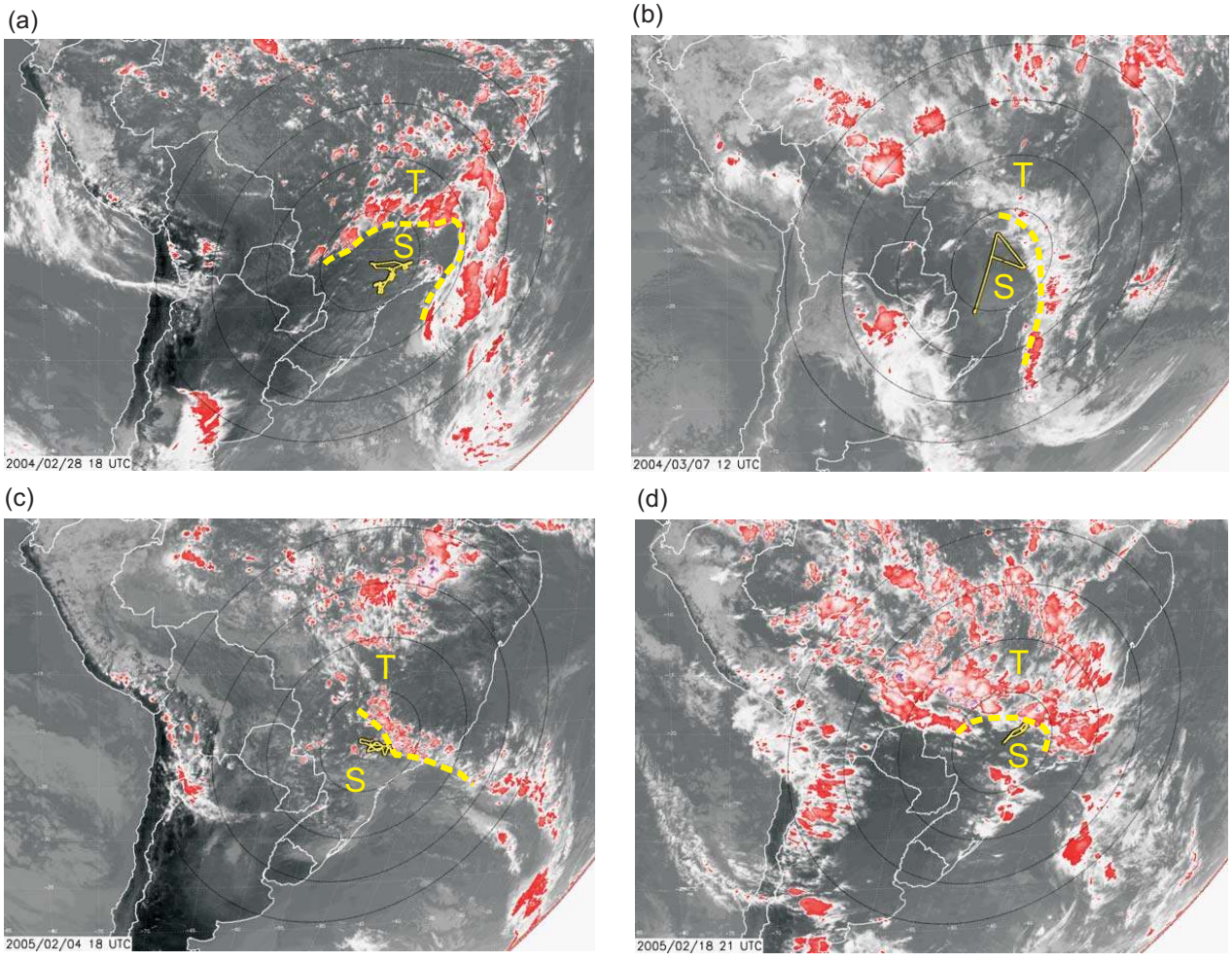

Fig. 3. GOES IR-images (brightness temperature, see colour bar in Fig. 7b) from **(a)** 28 February 2004 at 18:00 UTC, **(b)** 7 March 2004 at 12:00 UTC, **(c)** 4 February 2005 at 18:00 UTC, and **(d)** 18 February 2005 at 21:00 UTC. The Falcon flight track is superimposed in yellow (solid line). The position of the SACZ is also indicated in yellow (dashed line) separating tropical (T) and subtropical (S) air masses.

3.3.1 The Falcon flight on 28 February 2004

On 28 February 2004, especially high, average NO_x enhancements (compared to the background) were observed during repeated penetrations of the anvil of an active, isolated thunderstorm east of the operation centre (see also Table 2a). The SACZ was located more than 500 km away to the north and east. The investigated thunderstorm developed in a subtropical air mass with Θ_e temperatures between 334 and 344 K at 850 hPa, as calculated from Falcon data. This temperature range agrees well with the horizontal distribution of the Θ_e temperature at 850 hPa for this region, based on ECMWF data. The Falcon measurements indicate horizontal wind velocities in the UT between 20 and 30 m s^{-1} from the SW ($\sim$220°) influenced by the nearby subtropical jet, whereas the Bolivian High was located far away over NW Brazil and Bolivia. In addition, the main wind direction at 850 hPa was from the SW. In this case, all environmental parameters, see Table 2a, indicate that the air mass over the TROCCINOX observation area was purely subtropical. In agreement, CO mixing ratios in the mid troposphere were low (<50 nmol mol^{-1}), as indicated in Fig. 1b.

Only a few thunderstorms developed during the afternoon in the investigated area. A section of the Falcon flight is shown in Fig. 6a, as a thunderstorm with 20–30 km diameter was penetrated three times at different altitudes (10.7, 10.1 and 8.8 km) close to the thunderstorm centre. Based on brightness temperature, the thunderstorm reached an altitude of 11.5 km. Mean NO_x mixing ratios for the three anvil penetrations were about 1.4, 1.6, and 1.0 nmol mol^{-1}, respectively (see Table 2a and footnote[1]). The high NO/NO_y ratio of 0.7 to 0.8 indicates that NO was recently produced by lightning (not shown). CO mixing ratios in the anvil outflow were enhanced by 10–20 nmol mol^{-1} in comparison to

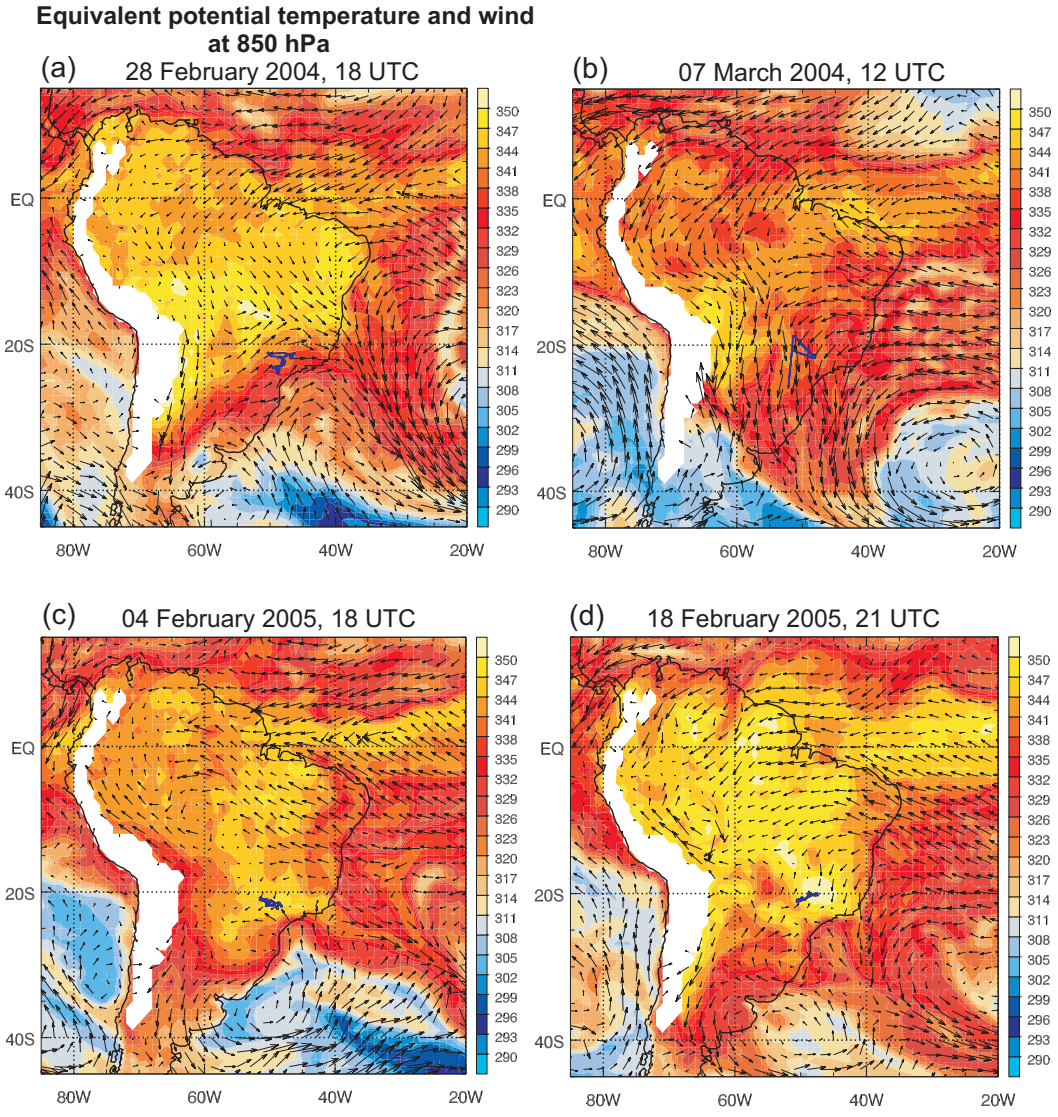

Fig. 4. Equivalent potential temperature (in K) and wind vector at 850 hPa for **(a)** 28 February 2004 at 18:00 UTC, **(b)** 7 March 2004 at 12:00 UTC, **(c)** 4 February 2005 at 18:00 UTC, and **(d)** 18 February 2005 at 21:00 UTC (based on ECMWF analyses). The Falcon flight track is superimposed.

the background ($\sim$50 nmol mol^{-1}), due to upward transport from the CO-richer BL (90–100 nmol mol^{-1}). The contribution from the BL to the measured anvil-NO_x was probably less than 0.2 nmol mol^{-1} (see Sect. 3.2, Figs. 1a–b). Thus, the mean LNO_x mixing ratio in the anvil outflow of this subtropical thunderstorm was estimated to $\sim$1.1 nmol mol^{-1}, contributing to more than 80% of total anvil-NO_x.

In addition, O_3 measurements are shown in Fig. 6a. However, the mixing ratios observed during the three anvil penetrations were very variable. During the first penetration, O_3 mixing ratios slightly decreased down to $\sim$50 nmol mol^{-1}, which can be explained by transport from the BL. However, during the second and third penetration of the same anvil at lower altitudes, O_3 mixing ratios strongly increased to values above $\sim$200 nmol mol^{-1}. We believe that these elevated O_3 signals are artificial, as discussed in Sect. 2.1. During the first and second anvil penetration we would expect about the same O_3 mixing ratios, since the increases in CO and NO_x mixing ratios are similar during these penetrations.

3.3.2 The Falcon flight on 7 March 2004

On 7 March 2004, an exceptionally widespread NO_x enhancement was sampled during $\sim$400 km of the flight (Table 2a). Note that this area was cloud-free during the measurements. The objective of this flight was to sample aged anvil outflow from a large MCS located 500–1000 km

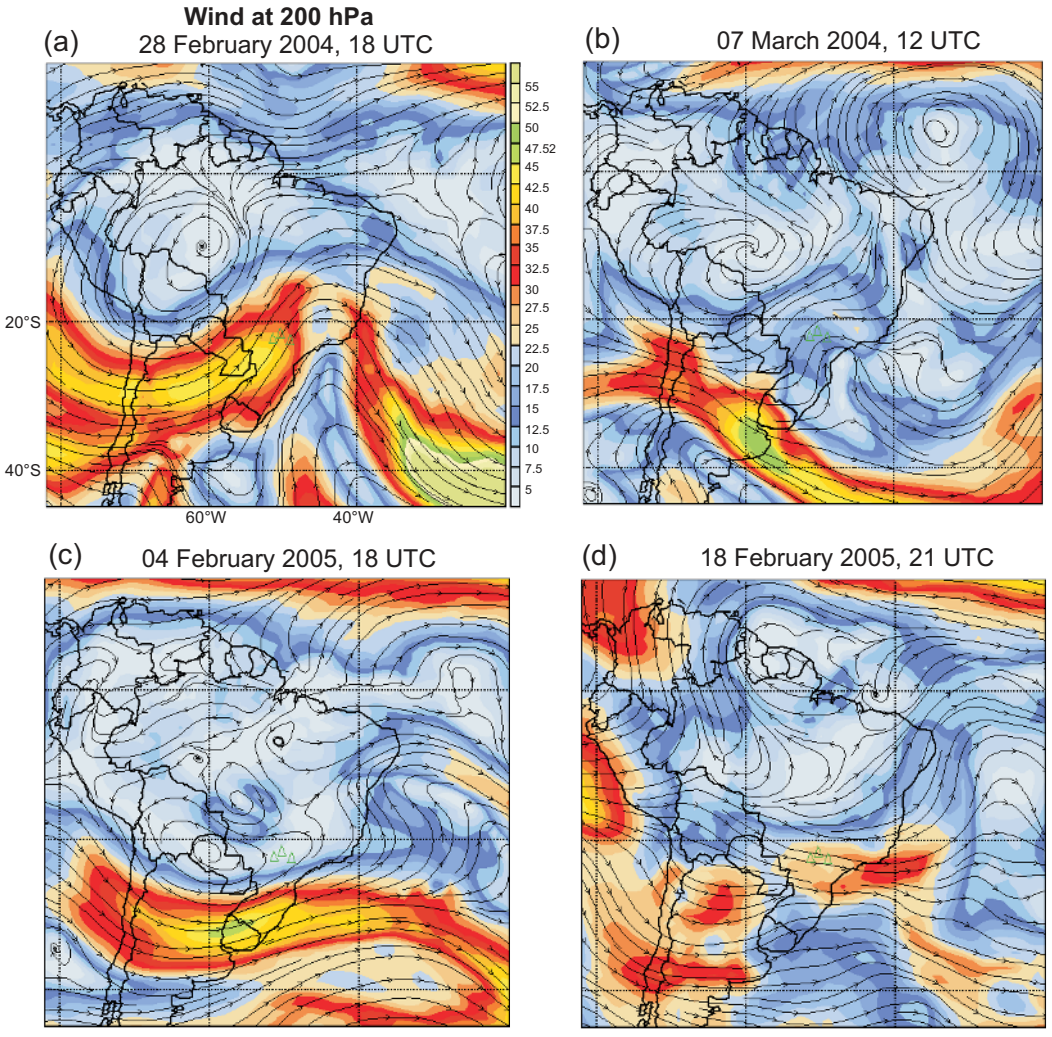

Fig. 5. Wind speed (in m s^{-1}) and stream lines at 200 hPa for **(a)** 28 February 2004 at 18:00 UTC, **(b)** 7 March 2004 at 12:00 UTC, **(c)** 4 February 2005 at 18:00 UTC, and **(d)** 18 February 2005 at 21:00 UTC (based on ECMWF analyses). The three triangles (in green) indicate the position of the two radars in Bauru (22.4° S, 49.0° W) and Presidente Prudente (22.1° S, 51.4° W), and the position of the airport in Aracatuba (21.1° S, 50.4° W).

Table 2a. Comparison of meteorological parameters and trace gas mixing ratios for selected flights in tropical and subtropical air masses.

Falcon Flight/ Tropical (t) or Subtropical (s)	Cloud Top Height, km (brightness temperature, K)	Pressure Altitude of Penetration, km	Mean Anvil-NO_x Mixing Ratio[1], nmol mol^{-1}	Anvil-NO_x Extension[2], km	CO Mixing Ratio at 500 hPa, nmol mol^{-1}	Equivalent Potential Temperature Θ_e at 850 hPa, K	South Atlantic Convergence Zone (SACZ)	Subtropical Jet	Bolivian High	Wind Velocity (Direction) in the UT, m s^{-1}	Wind Direction at 850 hPa
280204 (s)	~11.5 (220–225)	10.7 10.1 8.8	1.4 1.6 1.0	20–30	<50	334–344	>500 km away (N/E)	close-by (SW)	NW Brazil/ Bolivia	20–30 (SW)	SW
070304 (s) aged MCS[3]	~13 (210–215)	9–11	0.86±0.21[4]	400	40–50	338–352	~100 km away (N/E)	N-Argentina	NW Brazil/ Bolivia	10–25 (SSW)	NNE
040205 (t)	~16 (195–200)	10.6 10.7 10.1	0.87 1.20 0.68	20–40	80–90	347–353	in situ	Uruguay	Paraguay	5–10 (ENE/SW)	NE/SE
180205b (s)	~13 (210–215)	10.7 10.1 9.4	0.29/0.53[5] 0.32/0.76[5] 0.24/0.50[5]	30–40	50–60	342–352	close-by (N)	close-by (SE)	NW Brazil	15–25 (WNW)	SW

[1]The mean anvil-NO_x mixing ratio is the mean of all NO_x-values measured between the entrance and exit of the anvil at a given pressure altitude.
[2]The anvil-NO_x extension is the extension in flight direction, between anvil entrance and exit, perpendicular to the anvil outflow direction.
[3]Mesoscale Convective System.
[4]Due to the large extension of the anvil-NO_x enhancement from the MCS, the standard deviation is also given.
[5]Right value estimated from penetration close to the thunderstorm centre and left value estimated from penetration ~30 km further downwind.

Table 2b. Comparison of meteorological parameters for selected flights in tropical and subtropical air masses (mean values for the lowest 100 m layer).

Flight	Tropical (t) or Subtropical (s)/ Take off (TO) or Landing (L)	Pressure p, hPa	Temperature T_K, K	Relative Humidity U,%	Mixing Ratio r, g kg^{-1}	Potential Temperature Θ, K	Equivalent Potential Temperature Θ_e, K	Temperature at the Lifting Condensation Level (LCL) T_L, K	Pressure Altitude for LCL, km	Pressure Altitude for 0°C, km
280204	s/TO (0.6–0.7 km)	936	301	48	12.2	307	344	286	2.2	4.2–4.4
040205	t/TO (0.4–0.5 km)	963	299	86	19.5	302	360	296	0.8	4.7–4.8
040205	t/L (0.4–0.5 km)	960	299	66	14.9	303	347	291	1.3	4.7–4.8
050205	t/TO (0.4–0.5 km)	963	303	59	16.3	306	356	292	1.6	4.7–4.8
180205a	s/TO (0.4–0.5 km)	960	307	37	13.0	311	351	287	2.5	4.7–4.8
180205a	s/L (0.4–0.5 km)	958	307	33	11.9	311	348	284	2.8	4.7–4.8
180205b	s/TO (0.4–0.5 km)	960	308	37	13.5	312	353	287	2.6	4.9–5.2
180205b	s/L (0.4–0.5 km)	959	306	38	12.8	310	349	286	2.5	4.9–5.2

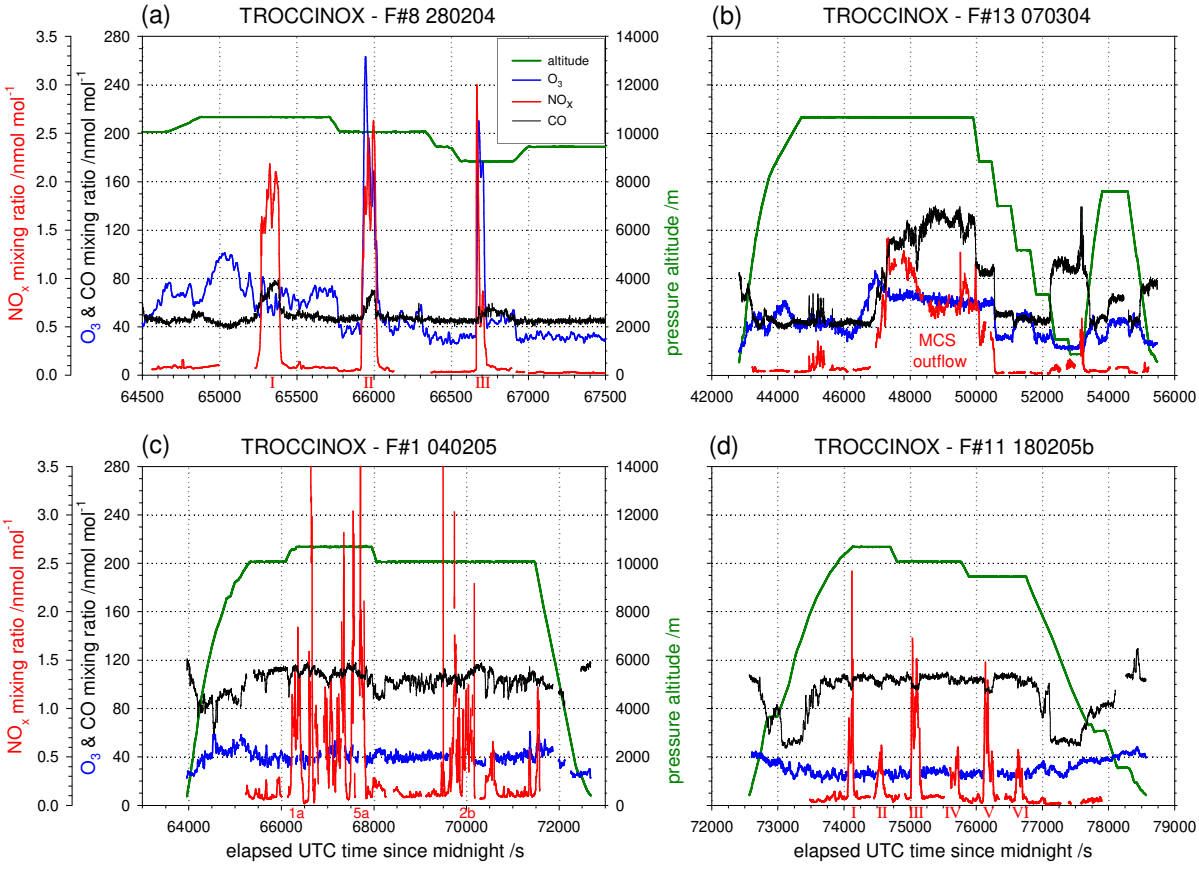

Fig. 6. Time series of NO_x, CO, O_3 and pressure altitude for the Falcon flights on **(a)** 28 February 2004, **(b)** 7 March 2004, **(c)** 4 February 2005, and **(d)** 18 February 2005 (all figures same y-axis ranges). Anvil penetrations are labelled. The elevated O_3 mixing ratios (up to 263 nmol mol^{-1}) measured during some of the anvil penetrations on 28 February 2004 (labelled II and III) are believed to be artificial (see Sect. 2.1 and 3.3.1).

upwind over northern Argentina and Paraguay at the time of the flight (Fig. 7b). The convective system developed one day earlier over NE Argentina and Uruguay (Fig. 7a). Forecasts from the ECHAM5/MESSy model of the horizontal LNO_x distribution at 300 hPa on 7 March indicate an extended area with elevated LNO_x moving rapidly north-eastward between 00:00 UTC and 12:00 UTC (Figs. 8a–b). Within these 12 h the LNO_x plume moved about 700 km, which corresponds to a velocity of 60 km h^{-1} and the maximum LNO_x mixing ratio in the model forecast decreased from ~2 to ~1 nmol mol^{-1}. At the time of the Falcon flight (11:53:49–15:24:33 UTC) this area extended towards the south-western part of the flight track as indicated in Fig. 2b.

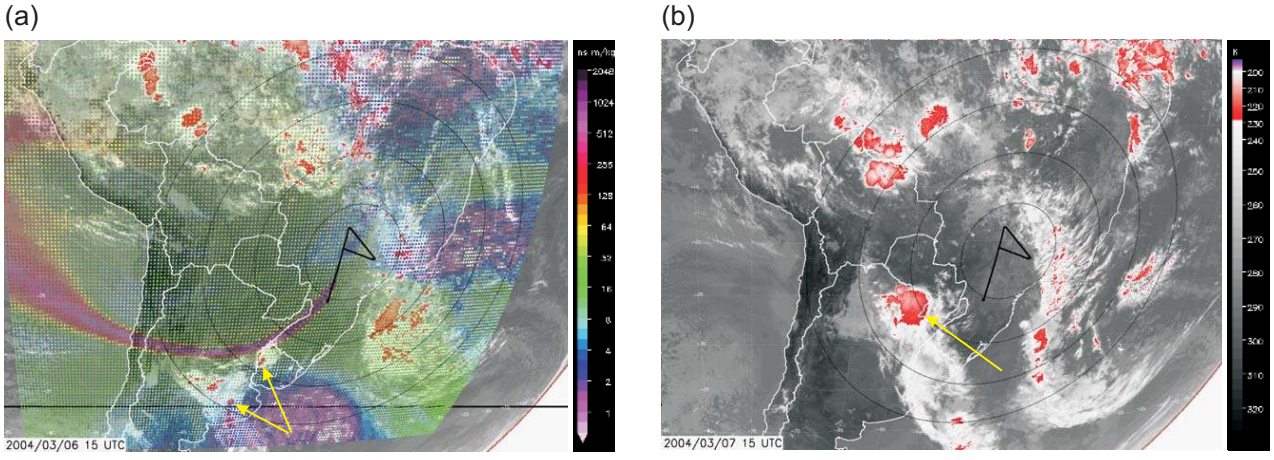

Fig. 7. Initiation and development of a MCS over northern Argentina, Uruguay and Paraguay on 6 **(a)** and 7 **(b)** March 2004 at 15:00 UTC. In the GOES IR-images (brightness temperature) the complete Falcon flight track (black) from 7 March is superimposed. In **(a)** FLEXPART backward simulations (colour scale) from the flight on 7 March are in addition superimposed indicating the source region of the investigated air mass (outflow from MCS over northern Argentina and Uruguay on 6 March, ∼24 h prior to the flight). The yellow arrows indicate the position of the developing MCS **(a)** and the MCS in the mature stage **(b)**.

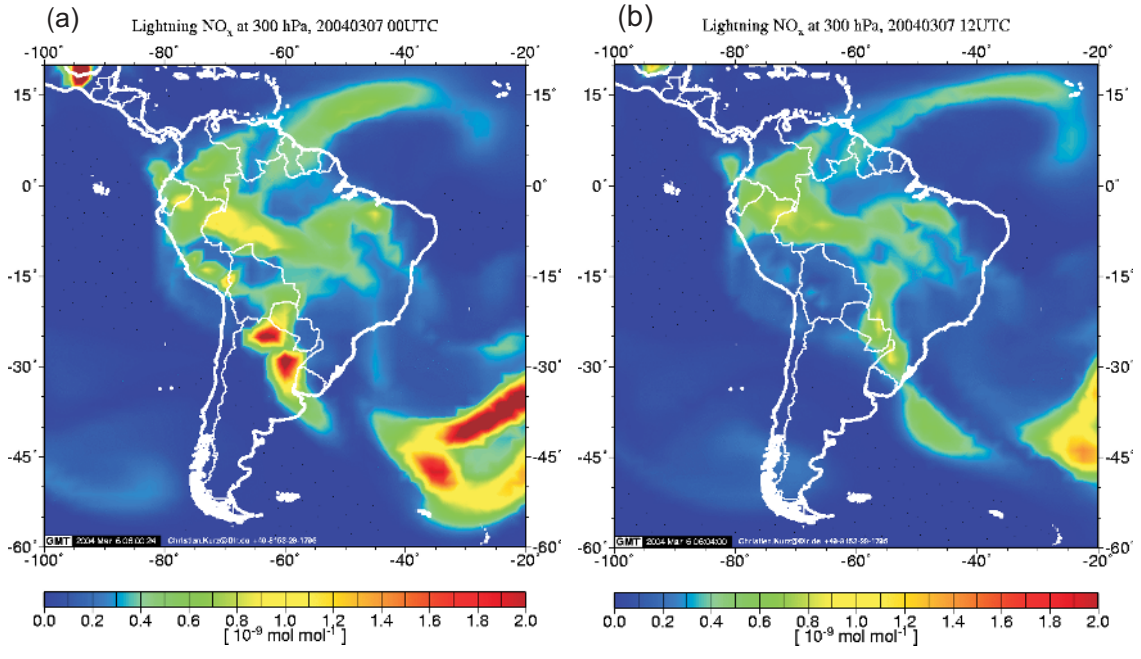

Fig. 8. ECHAM5/MESSy model forecasts of LNO_X at 300 hPa for 7 March 2004, 00:00 UTC **(a)** and 12:00 UTC **(b)**.

On this day, the SACZ was located to the north and east as in the previous case, however rather close to the observation area (∼100 km). Calculated Θ_e temperatures at 850 hPa from Falcon data varied between 338 and 352 K (compare to ECMWF analyses). Elevated horizontal winds of 10 to 25 m s^{-1} from the SSW (∼200°) measured by the Falcon dominated in the UT (compare to ECMWF analyses). At 850 hPa, the winds came from the opposite direction (NNE), indicating advection of different air mass types at different levels. The advection of warm and humid air masses from the Amazon basin with a low-level jet is a typical situation for generation of MCS in southeastern South America (Salio et al., 2007). The MCS developed further to the SW, along a transition zone between northerly and southerly low level

winds. The Bolivian High was located far away over NW Brazil and Bolivia. In this case, the meteorological parameters, see Table 2a, indicate that the air mass over the TROCCINOX observation area was predominantly subtropical, except for the advection of tropical air masses with elevated Θ_e in lower levels from the north (Amazon basin). In agreement, CO mixing ratios in the mid troposphere were low (40–50 nmol mol^{-1}), as indicated in Fig. 1b.

Similar situations, with the observation area being located downstream of a large MCS, were observed on further days during TROCCINOX, e.g. 1 and 7–8 February 2005. Chemical measurements in the vicinity of South American MCS are rare (Velasco and Fritsch, 1987; Pickering et al., 1996; Smyth et al., 1996). Therefore, the features of the flight of 7 March 2004 are presented here in more detail. The 1 and 8 February 2005 cases are discussed in more detail by Konopka et al. (2006), where signatures of a deep stratospheric intrusion into the TTL (tropical tropopause layer) and troposphere-to-stratosphere transport along the subtropical jet were observed.

On 7 March 2004, enhanced NO_x, CO and O_3 mixing ratios in the range of 0.6–1.1, 110–140 and 60–70 nmol mol^{-1}, respectively, were sampled over a wide distance of 400 km (from 21° S to 25° S along 52° W), between 9 and 11 km altitude in the aged anvil outflow (Figs. 2b and 6b). The rather low and constant NO/NO_y ratio of 0.2 to 0.4 indicates that aged, well-mixed NO emissions were probed (not shown). The NO_y mixing ratio in the aged anvil outflow was high (~2.0–2.5 nmol mol^{-1}), indicating a strong source. The average NO_x mixing ratio in the aged MCS outflow of about 1 nmol mol^{-1} is close to the average value observed in fresh TROCCINOX thunderstorms (see Table 2a), however in this case the BL-NO_x contribution was likely larger.

Backward simulations with the Lagrangian particle dispersion model FLEXPART from a flight section on 7 March (Fig. 7a) indicate that the observed NO_x-rich air mass was advected within ~1 day from a MCS located over the Buenos Aires area on 6 March. Pollution from this urban area was probably uplifted by the system, which partly might explain the elevated CO and NO_x mixing ratios observed. In addition, emissions from fires might have been uplifted, since just ahead of the MCS widespread vegetation fires over Paraguay and Uruguay were observed in the time period 2-7 March 2004 from space by MODIS (Moderate Resolution Imaging Spectroradiometer) (Fig. 9). For general information on the MODIS Rapid Response fire locations see, e.g. Justice et al. (2002), Giglio et al. (2003), Davies et al. (2004), and http:www.//maps.geog.umd.edu/.

For the same region and period, satellite observations of CO at 850 Pa from the MOPITT (Measurements Of Pollution In The Troposphere) instrument on 2 March show a large area with enhanced CO in the BL (Fig. 10a) and an elevated CO area in 150 hPa further to the north (Fig. 10b). For general information on MOPITT see, e.g. Drummond and Mand (1996), Edwards et al. (1999), and http://www.eos.ucar.edu/mopitt/. In addition, tropospheric NO_2 from the SCIAMACHY (SCanning Imaging Absorption spectroMeter for Atmospheric CHartographY) instrument on 3 March show a large area with enhanced NO_2 over Paraguay (Fig. 11a), presumably mainly from biomass burning (compare Fig. 10a and Fig. 11a to Fig. 9). For general information on SCIAMACHY see, e.g. Burrows et al. (1995), Bowensmann et al. (1999), and http://www.iup.physik.uni-bremen.de/sciamachy/. For pixels with less than 20% cloud cover, a clear sky air mass factor was used as described in (Richter et al., 2005). For scenes with a larger cloud fraction, an air mass factor appropriate for a NO_2 layer above a thick cloud was used (Hild et al., 2002). No attempt was made to correct for mixed pixels or for NO_2 below the cloud. Therefore, the values obtained are representative for NO_2 above the clouds and in the cloud top, where the measurement sensitivity is large but do not include boundary layer NO_2 in cloudy situations.

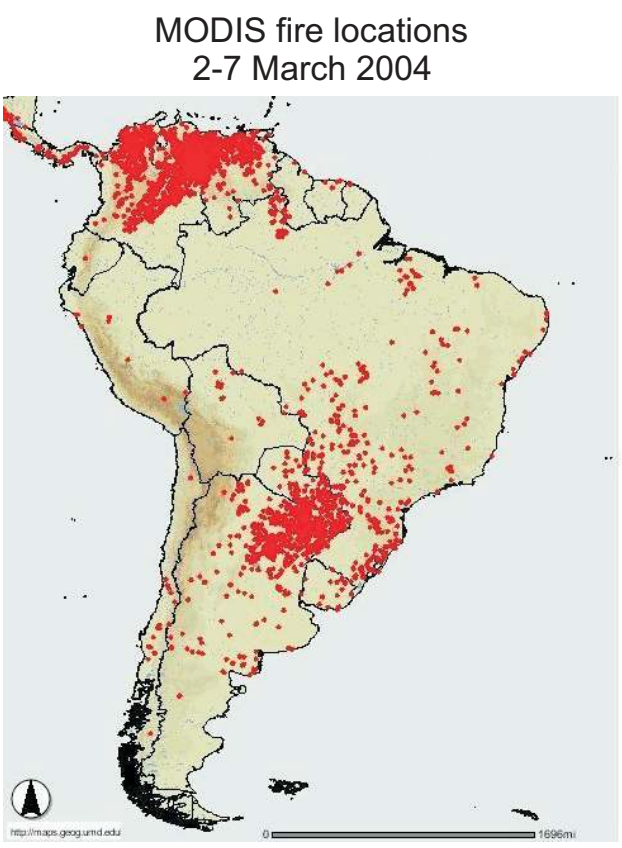

Fig. 9. MODIS fire locations (in red) over South America for the time period 2–7 March 2004 indicating enhanced fire activity over northern Argentina and Paraguay. (MODIS-map from: http://maps.geog.umd.edu/)

In Fig. 11b the extension of enhanced NO_2 in the vicinity of the MCS at 13:30 UTC on 7 March roughly agrees with the extension of LNO_x at 300 hPa in the ECHAM forecast for 12:00 UTC (Fig. 8b). The extension in the N-S direction

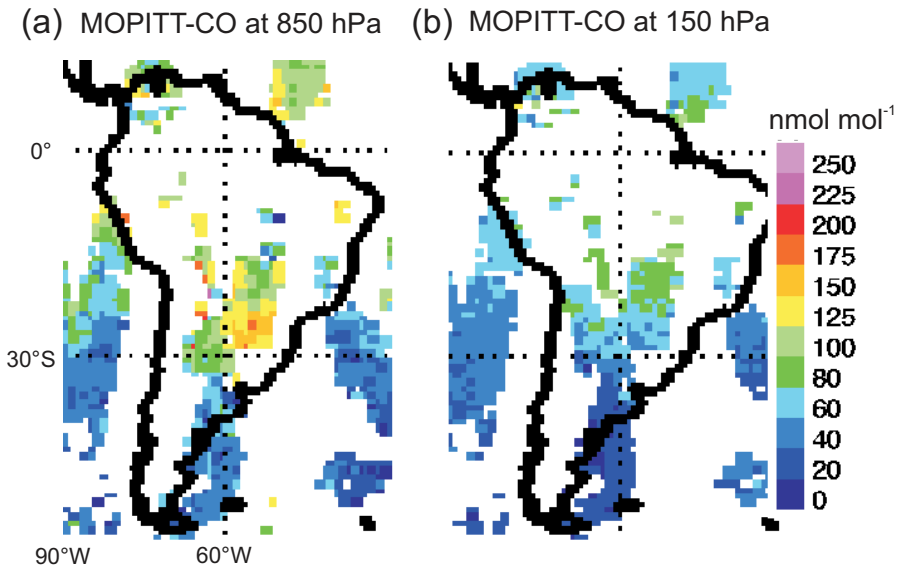

Fig. 10. Global distribution of CO at 850 hPa **(a)** and 150 hPa **(b)** derived from MOPITT on 2 March 2004. Over northern Argentina and Paraguay, CO was enhanced at 850 hPa (a) from biomass burning (see Fig. 9). (MOPITT-Maps from: http://www.eos.ucar.edu/mopitt/data/index.html)

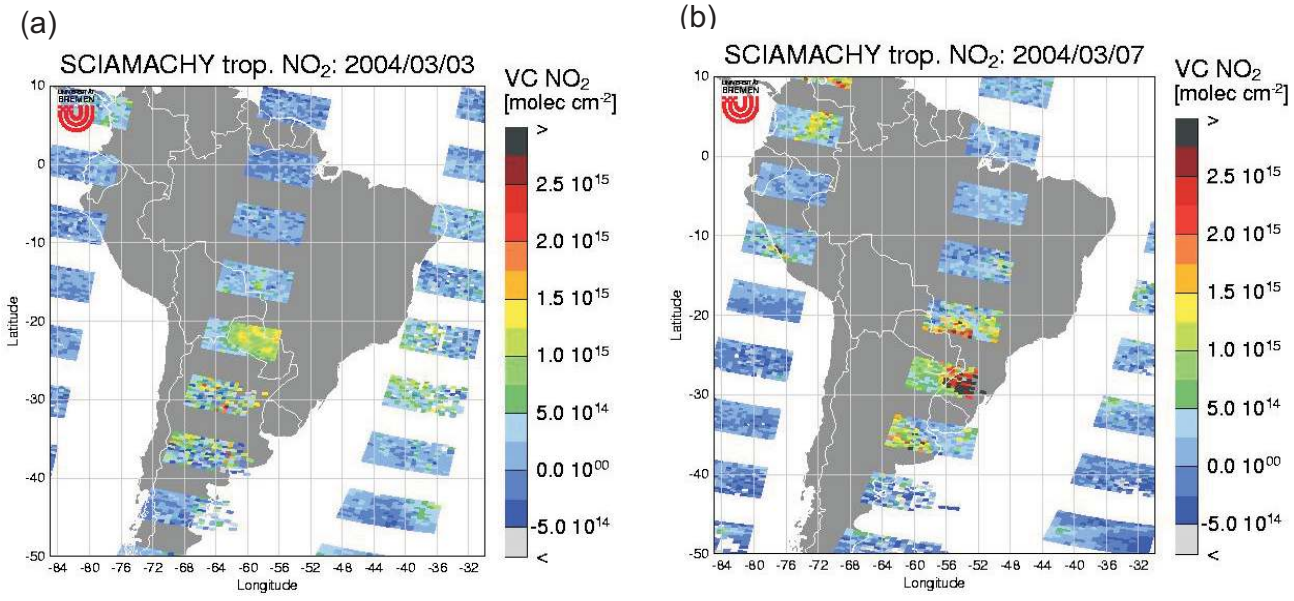

Fig. 11. Tropospheric NO_2 over South America derived from SCIAMACHY measurements on 3 **(a)** and 7 **(b)** March 2004 at 13:30 UTC. A standard air mass factor was used and it was distinguished between cloudy and non-cloudy pixels. Over northern Argentina, Paraguay and SW Brazil, the tropospheric NO_2 column was enhanced; on 3 March presumably due to emissions from biomass burning in the BL and on 7 March due to uplifted emissions from both biomass burning, lightning and urban pollution in the outflow of an aged MCS.

is about 800 km and in the E-W direction about 400 km. The Falcon measurements indicate a depth of the enhancement of ∼2 km. Downwind of the MCS, NO_x mixing ratios between 0.6–1.1 nmol mol^{-1} were measured by the Falcon aircraft which are in the same range as predicted in the LNO_x forecast, ∼1 nmol mol^{-1} (Fig. 8b). An estimate, based on the satellite observed NO_2 distribution in Fig. 11b (NO_2-column: 2.5×10^{15} molec. cm^{-2}) and an anvil outflow depth of 2 km,

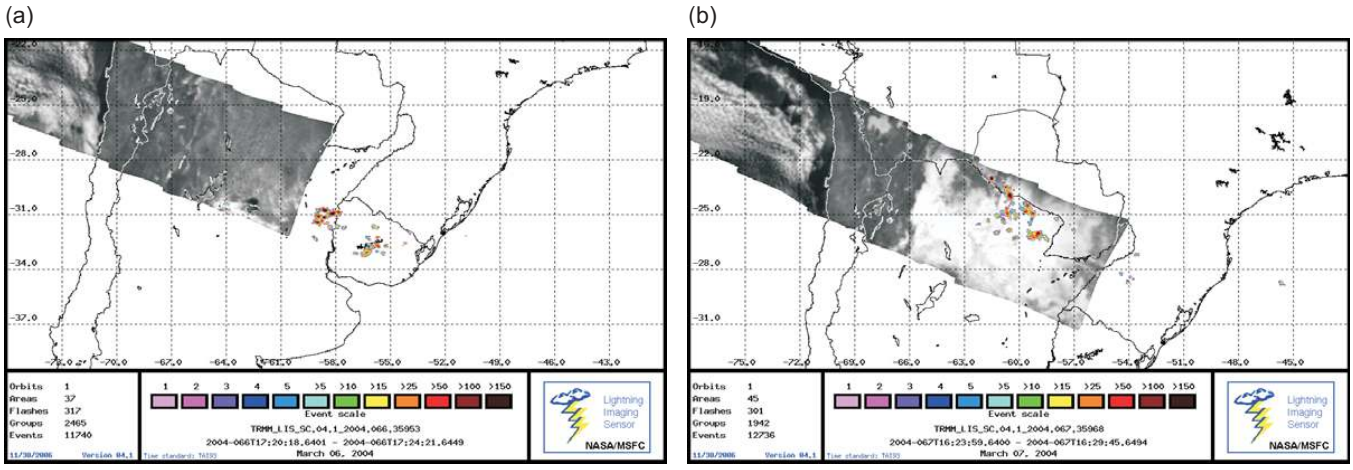

Fig. 12. LIS lightning events (colour scale gives number of lightning events) over northern Argentina, Uruguay, Paraguay and SW Brazil superimposed on a LIS background cloud-field image for **(a)** 6 and **(b)** 7 March 2004 when the TRMM satellite passed over this region in the afternoon (compare to Fig. 7). (LIS-Maps from: http://thunder.msfc.nasa.gov/).

give NO_2 mixing ratios in the range of 1.5 nmol mol^{-1}. This value is rather high, however the overall column depth of the outflow is probably larger than 2 km, which would decrease the estimated value.

Besides upward transport of emissions from biomass burning and urban pollution, presumably lightning in the MCS produced additional NO. Observations of an elevated number of lightning events in the MCS on 6 and 7 March are shown in Figs. 12a–b, as registered optically by the LIS instrument aboard the TRMM (Tropical Rainfall Measurement Mission) satellite (compare to cloud distribution in Figs. 7a–b). One or more adjacent lightning events in the same 2ms time frame can be bunched together to form a group. A flash consists of one or more groups sufficiently close in time and space (not shown here). For general information on LIS see, e.g. Christian et al. (1999), Thomas et al. (2000), Boccippio et al. (2002) and http://thunder.msfc.nasa.gov/lis/. On 6 March in the afternoon, lightning was centred in the MCS over Uruguay and its surroundings to the NW. On 7 March in the afternoon, the area with enhanced lightning activity in the MCS had moved to the north and was located west of Paraguay.

From these observations, we conclude that emissions from both biomass burning, lightning, and urban pollution presumably contributed to the elevated NO_x and CO mixing ratios observed in the MCS outflow. In addition, O_3 was elevated in the outflow, but no data are available to determine whether it was produced already at the ground or produced from precursors after transport to the UT. Furthermore, in Sect. 5 a possible influence from the O_3-rich upper troposphere – lower stratosphere (UTLS) region is discussed.

Only in this aged outflow from MCS, a pronounced O_3 enhancement was observed during TROCCINOX. Forward trajectories for six subsequent days were calculated to follow the O_3-rich air mass measured on 7 March 2004. The air mass was transported to the north and then to the west, slightly ascending to 150–200 hPa within the intertropical convergence zone (ITCZ), and circulated further westwards driven by the Bolivian High to a region between 20° S to 5° S and 80° W to 65° W (Fig. 13). Because of the presence of the Bolivian High, transport of the MCS outflow towards the equator and the subsequent circulation around the Bolivian High is probably a common feature over Brazil. Therefore, we suggest that emissions in the MCS outflow from distant urban pollution, lightning and biomass burning events may

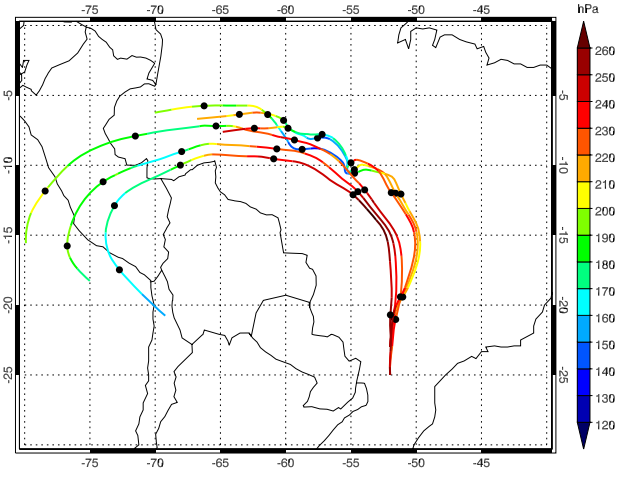

Fig. 13. Six days forward trajectories indicating the transport pathway of the MCS outflow from 7 March 2004, 15:00 UTC, into the Bolivian High. The black dots indicate the position of the air mass after 1 to 6 days of forward calculations. The colour bar gives pressure values (in hPa) along the forward trajectories.

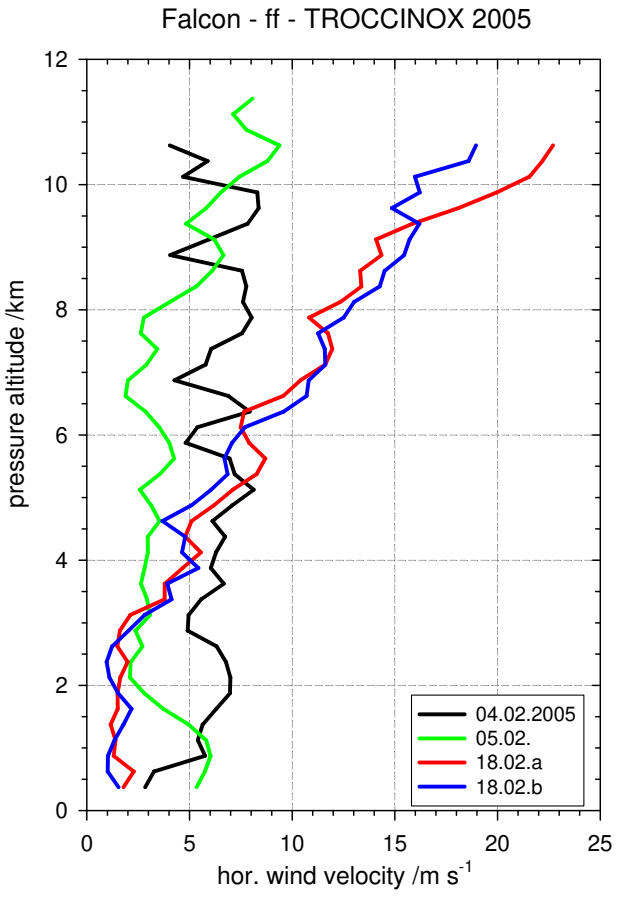

Fig. 14. Mean vertical profiles of the horizontal wind velocity derived from Falcon measurements in tropical (4–5 February 2005) and subtropical (18 February 2005) air masses. Mean values are given for every 250 m altitude bin.

have, in addition to local convectively uplifted sources emitted from the Amazon basin, an important impact on the tropical NO_x, CO and O_3 budget in and around the Bolivian High.

3.3.3 The Falcon flight on 4 February 2005

On 4 February 2005, tropical air masses with elevated Θ_e penetrated to the south and reached the TROCCINOX observation area, where many thunderstorms developed in the late afternoon and evening. The SACZ was located right over the area and a part of the Bolivian High was located closer than usual, to the west over Paraguay. Calculated Θ_e temperatures at 850 hPa from Falcon data were in the range of 347–353 K, indicating tropical air masses (compare to ECMWF analyses). Weak winds of 5 to 10 m s^{-1} from the eastnortheast and the southwest dominated in the UT according to Falcon measurements. The subtropical jet was displaced by the Bolivian High and located further to the south. At 850 hPa, the main wind direction in the northern part of the observation area was from the NE and in the southern part from the SE, indicating low-level convergence. The horizontal wind velocity was almost constant with altitude and weak, which seems to be typical for air masses within the Bolivian High, see Figs. 5c and 14 (here data from a further flight, 5 February 2004, was also included). Both the high Θ_e values of more than 345 K at 850 hPa and the weak winds in the UT from northerly and easterly directions indicate a difference between these tropical air masses and the subtropical air masses described before (Table 2a). CO mixing ratios in the mid troposphere were elevated to 80–90 nmol mol^{-1}, as indicated in Fig. 1b, supporting the origin of the air masses from the tropical region in the north.

Widespread tropical deep convection developed in the afternoon after 17:00 UTC (Figs. 3c, 15a). Most systems were short-lived (∼1 h) due to weak horizontal winds and little shear, and they were rather narrow (20–40 km). Because of the rapid pulse-like development of this type of very deep convection, it was difficult to direct the Falcon aircraft. In addition, due to the widespread occurrence of deep convection, visibility was poor during the flight. The Falcon was directed to different developing thunderclouds from the operation centre, but had to fly around intense convection resulting in a zigzag pattern at altitudes between 10.1 and 10.7 km and repeated penetrations of single tropical thunderstorms were almost not possible. However, single penetrations of these tropical thunderstorms succeeded several times and three of the penetrations (labelled 1a, 5a and 2b in Figs. 2c, 6c) were selected to be presented in more detail in a forthcoming paper (Huntrieser et al., 2007[1]).

In Fig. 6c the distributions of CO, O_3, and NO_x mixing ratios along the Falcon track on 4 February 2005 are shown. Reliable O_3 measurements are not available for the anvil penetrations for reasons discussed before (see Sect. 2.1). Two periods with thunderstorm penetrations are visible at 66 000–68 000 s (=18:20–18:53 UTC) and at 69 500–70 000 s (=19:18–19:27 UTC). Mean NO_x mixing ratios during these turbulent penetrations in vicinity of the thunderstorm lightning centre were in the range of 0.6–1.0 nmol mol^{-1}, similar to the previous observations (Table 2a), however background NO_x mixing ratios were slightly higher than in the subtropical air masses. Narrow, high NO peaks of up to 8 nmol mol^{-1}indicate recent production by free tropospheric lightning. Though, we cannot exclude that such isolated peaks are measurement artefacts caused by discharges on the aircraft fuselage or inlets as suggested by Ridley et al. (2006). In this tropical air masses, background CO mixing ratios in the UT were as high as in the BL (almost 120 nmol mol^{-1}). Therefore, during the anvil penetrations there was no clear enhancement in CO mixing ratios above the background. In comparison, O_3 mixing ratios in the free tropospheric background were low (∼40 nmol mol^{-1}).

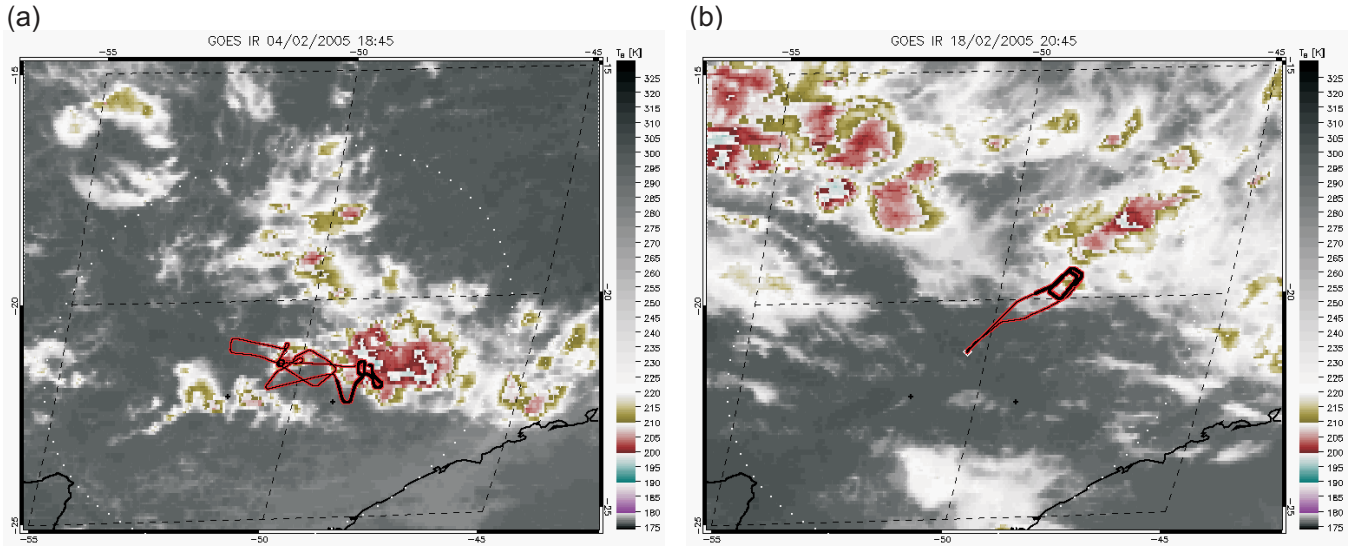

Fig. 15. GOES IR-images (brightness temperature in K) indicating the penetration of selected thunderstorms on **(a)** 4 and **(b)** 18 February 2005 with the Falcon flight track (black-red) superimposed. The thick part of the flight track indicates a time period of 30 min, 15 min prior and after the time given for the satellite image.

3.3.4 The Falcon flight on 18 February 2005

On 18 February 2005, the SACZ touched the TROCCINOX area in the north and a flight was performed to the northeast. Calculated Θ_e temperatures at 850 hPa from Falcon data reached values between 342 and 352 K (compare to ECMWF analyses). The centre of the Bolivian High was located far to the northwest over Brazil, and a branch of the subtropical jet was in vicinity to the east. Strong winds from WNW of 15–25 m s^{-1} were observed in the UT by the Falcon aircraft (Fig. 14). At 850 hPa, the main wind direction was from the SW. In this case, the observations indicate that the air mass over the TROCCINOX observation area was predominantly subtropical (Table 2a), except for the presence of tropical air masses with elevated Θ_e in some areas at 850 hPa and tropical air masses in the UT (see detailed discussion of CO mixing ratios further below). As expected for subtropical air masses, CO mixing ratios in the mid troposphere were rather low (50–60 nmol mol^{-1}), as indicated in Fig. 1b.

In the northern part of the TROCCINOX observation area (20° S, 48° W) a long-lived thunderstorm system developed in the afternoon (Fig. 15b). The system was long-lived probably because of the pronounced wind shear (Fig. 14). The system, with a diameter of 30 to 40 km, was penetrated six times by the Falcon aircraft at the altitudes 10.7, 10.1, and 9.4 km (Fig. 2d). On each level, one penetration ~10–30 km downwind from the thunderstorm lightning centre and another penetration ~30 km further downwind were performed. In Fig. 15a–b the cloud top brightness temperature indicates that the cloud top height of this subtropical thunderstorm system on 18 February (~13 km, 210–215 K) was lower in comparison to the investigated tropical thunderstorms on 4 February 2005 (~16 km, 195–200 K).

During the 18 February 2005 flight, CO mixing ratios showed large differences between the mid and upper troposphere (50 and 110 nmol mol^{-1}, respectively), as shown in Fig. 1b and 6d. FLEXPART backward simulations over 20 days indicate a distinct difference in the air mass origins (Fig. 16a–b). The air masses in the mid troposphere with low CO mixing ratios (and low H_2O, shown in Sect. 4) were rapidly transported from the subtropical mid Pacific. The air masses in the UT with high CO (and high H_2O) mixing ratios had a tropical origin in the Amazon basin and circulated around the western side of the Bolivian High. This was a common situation observed on many TROCCINOX flights and explains the wide separation between the vertical CO profiles presented in Fig. 1b. Conversely, no strong differences in the O_3 mixing ratios were observed between the Pacific and Amazon basin air masses (Fig. 6d). Background O_3 mixing ratios for both air mass types were low and varied between 20 and 40 nmol mol^{-1}.

During the repeated thunderstorm penetrations, NO_x mixing ratios were distinctly elevated in the anvil outflow with means between 0.2 and 0.8 nmol mol^{-1}, however less than in the previous cases discussed (Table 2a). CO mixing ratios slightly decreased to 95–100 nmol mol^{-1} compared to the ambient UT with 105–110 nmol mol^{-1}, indicating upward transport from the upper part of the BL with lower CO mixing ratios in the range of 80–100 nmol mol^{-1}.

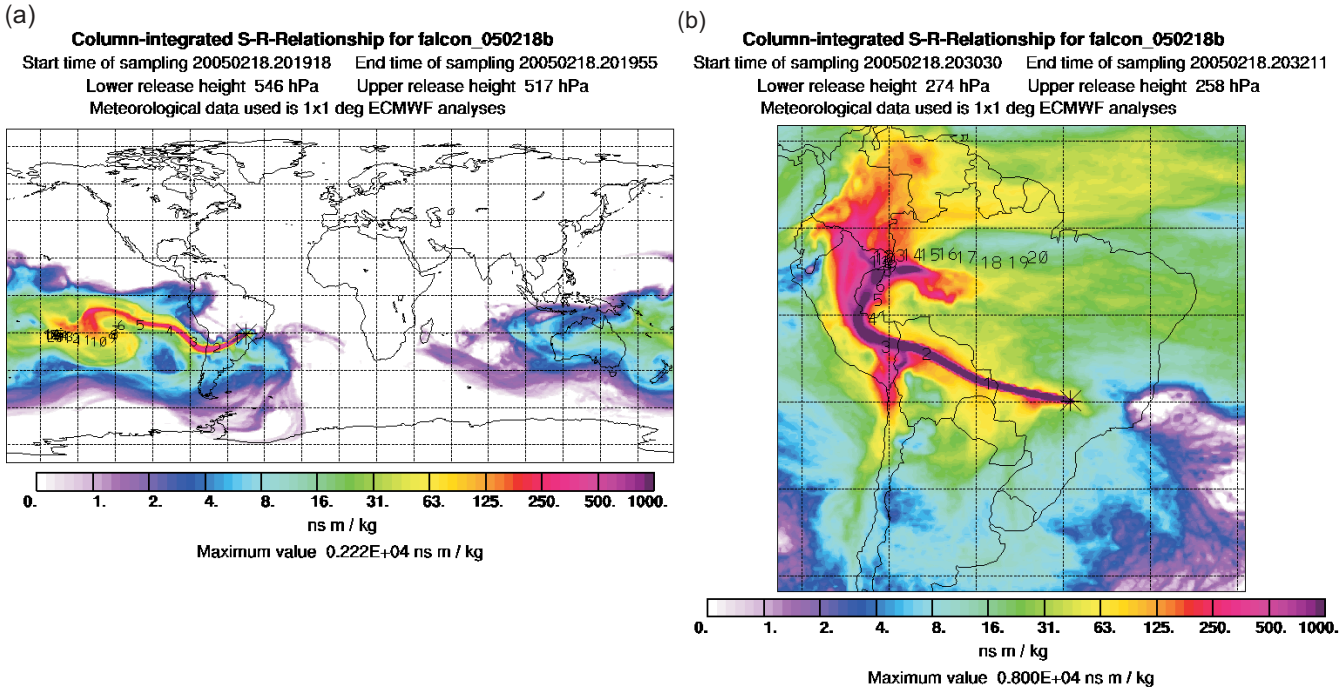

Fig. 16. FLEXPART column-integrated source-receptor relationship indicating the transport pathway (colour) and transport age in days (numbers) of an air mass investigated by the Falcon aircraft on 18 February 2005, **(a)** 20:19:18–20:19:55 UTC (subtropical origin) and **(b)** 20:30:30–20:32:11 UTC (tropical origin).

4 Vertical distribution of temperature and humidity in tropical and subtropical air masses

Further differences between tropical and subtropical air masses are also prominent from the meteorological parameters listed in Table 2b. The flight from 7 March 2004 is not included here, since no representative initial conditions for the MCS over northern Argentina are available. All input parameters for the calculation of the potential temperature (Θ), and of Θ_e and T_L, as described in Sect. 3.2, (Eqs. 1 and 2), are listed in Table 2b. The values represent averages of the lowest 100 m layer of the atmosphere at take-off or landing.

In the tropical air masses on 4 and 5 February 2005, the temperature was lower but the relative humidity and H_2O mixing ratio were higher than in the subtropical air masses on 28 February 2004 and 18 February 2005. As a result, the Θ_e and T_L temperatures were mostly higher. The lifting condensation level was reached earlier at ~1–1.5 km, in comparison to subtropical air masses at ~2–3 km, which may influence the vigour of convection and the occurrence of lightning according to Mushtak et al. (2005) (see further discussions in a forthcoming paper, Huntrieser et al., 2007[1]). The pressure altitude of the 0°C level was within the same range. These findings from a few tropical cases (Table 2b) indicate, that more cloud droplets may fall out of tropical deep convection, because they condensate at a lower cloud base and therefore grow to larger sizes before they reach the freezing level. As a result, less supercooled liquid water is available, which is essential for the charge separation (Williams et al., 2002; Cecil et al., 2005). It has been observed that the precipitation in deep convection over tropical Brazil (Amazon) is more of a maritime type (so-called "warm rain" without significant ice scattering signatures) (Williams et al., 2002).

Further differences between tropical and subtropical air masses are also prominent in the vertical temperature and water vapour profiles, as shown in Figs. 17a–b. In pronounced subtropical air masses on 28 February 2004, temperatures measured in the lowest 1 km are similar to those in the tropical air masses on 4 February 2005. However, more moisture is available in the tropical air masses, which supports the development of clouds with lower cloud base. Furthermore, the temperature lapse rate in the lowest 3 km is lower (almost moist adiabatic) in tropical air masses than in subtropical air masses. The elevated H_2O mixing ratios throughout the troposphere indicate a well mixed tropical air mass. In contrast, on 18 February 2005 a dry layer originating from the subtropical mid Pacific is prominent in the mid troposphere.

In addition, vertical profiles of Θ and Θ_e temperatures are shown in Figs. 17c–d, respectively. The Θ temperature in the BL is similar on 28 February 2004 (subtropical air mass case) as on 4 February 2005 (tropical air mass case). However, above the BL this temperature increases more strongly with altitude in the tropical than in the subtropical air mass.

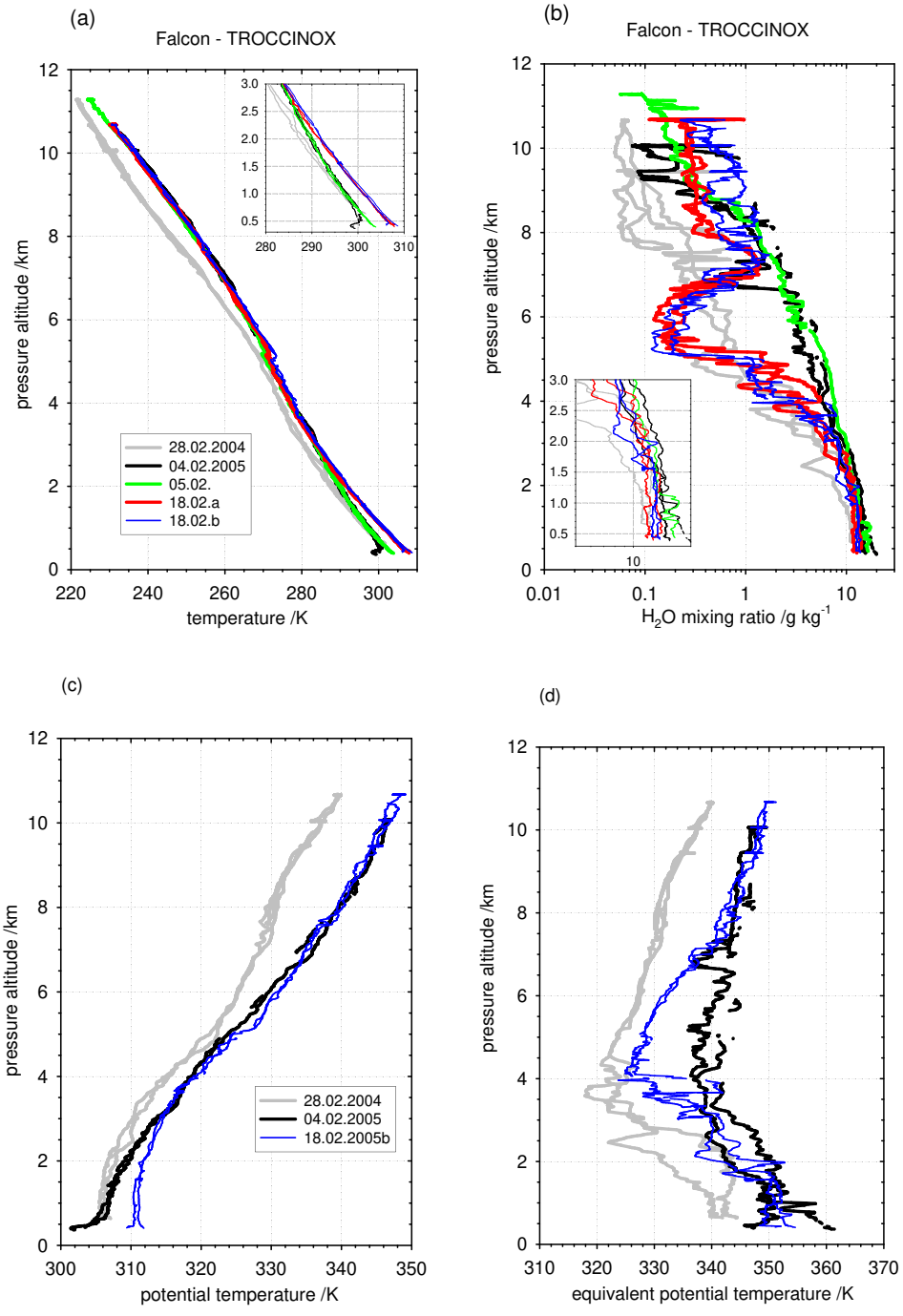

Fig. 17. Vertical profiles (1 s values) for temperature **(a)**, H_2O mixing ratio **(b)**, potential temperature Θ **(c)**, and equivalent potential temperature Θ_e **(d)** derived from Falcon measurements for tropical (4–5 February 2005) and subtropical (28 February 2004 and 18 February 2005) air masses. In **(a)** and **(b)** the lower part of the profile (up to 3 km) is shown enlarged in the insets.

In addition, the vertical distribution of the Θ_e temperature indicates distinct differences between tropical and subtropical air masses. In the subtropical air mass, the Θ_e temperature is about 10 to 20 K lower than in the tropical air mass. The third case presented in Figs. 17c–d, 18 February 2005, is of mixed nature. The SACZ is located close to the observation area, which is also reflected in the elevated Θ_e temperatures in the BL and UT. However, the low Θ_e temperature of the mid troposphere still indicates the influence of cool and dry subtropical air masses. For this reason, the Θ_e temperature at

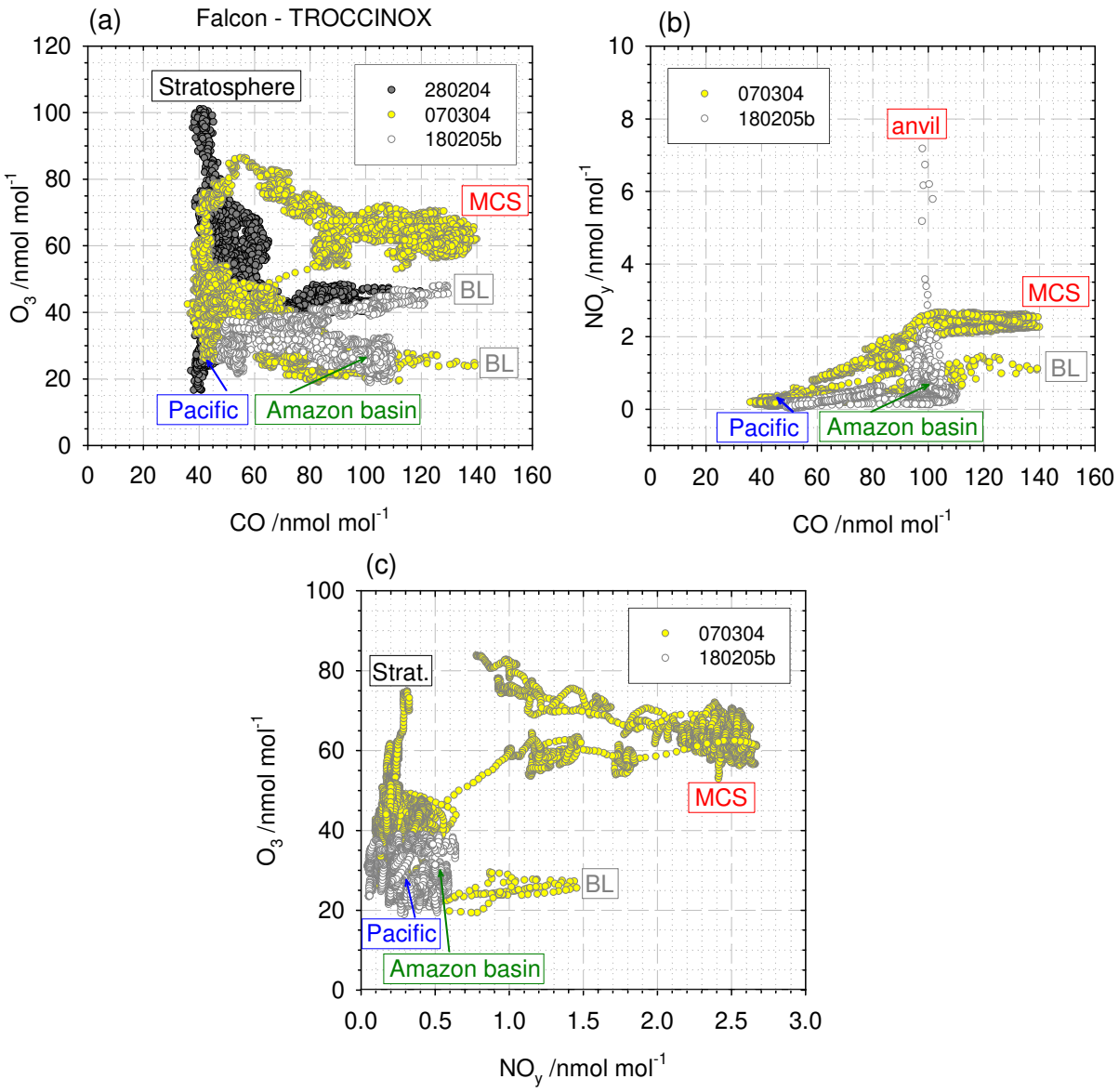

Fig. 18. Correlation plots for **(a)** O_3-CO, **(b)** NO_y-CO, and **(c)** O_3-NO_y derived from Falcon measurements on 28 February 2004 (grey), 7 March 2004 (yellow), and 18 February 2005 (white dots). Different types of air masses are labelled.

500 hPa was used as an additional criterion to separate tropical and subtropical air masses (see Sect. 3.2), which is in accordance with previous findings by Pickering et al. (1993) during ABLE 2A (dry season) and ABLE 2B (wet season) over the Amazon basin in Brazil (see Fig. 10 in their paper). Pickering et al. (1993) also pointed out, that this cool and dry layer in the mid troposphere is important to retain intense thunderstorms for several hours. In addition, the vertical Θ_e profiles in Fig. 17d show similar Θ_e temperature in the BL as in the UT. In agreement with Highwood and Hoskins (1998) and Folkins et al. (2000), this indicates efficient vertical cloud formation and transport.

5 Trace gas correlations in tropical and subtropical air masses

The different air mass types which were penetrated by the Falcon aircraft are reflected in different trace gas correlations, see Figs. 18a–c. Here only the data for flights with pronounced signatures in the trace gas correlations are shown (narrow correlations and/or distinct air mass signatures) to avoid too much scatter. CO, O_3, and NO_y data from the flights on 28 February 2004 (grey dots), 7 March 2004 (yellow dots) and 18 February 2005 (b-flight) (white dots) were selected for Fig. 18a and only data from the latter two flights for Figs. 18b–c. The different air mass origins are labelled (branches in correlation plot).

Tropical air masses typically originated from the continent, the Amazon basin, and were frequently trapped within or at the edge of the Bolivian High (Fig. 16b). Subtropical air masses typically originated further away above the Pacific Ocean (Fig. 16a). As discussed before, both of these air mass types were characterised by low O_3 mixing ratios of 20 to 40 nmol mol^{-1}, see Fig. 18a. In the Pacific air mass, O_3 and CO was positively correlated and CO mixing ratios were low in the range of 40–60 nmol mol^{-1} (pronounced on 28 February 2004 and slightly visible on 7 March 2004 and 18 February 2005). In comparison, the air mass originating from the Amazon basin contained elevated CO in the range of 80–110 nmol mol^{-1}, and O_3 and CO was negatively correlated (pronounced in the UT on 18 February 2005 and in the BL on 7 March 2004).

During ascent and descent in the BL, a positive O_3-CO correlation, probably due to photochemical O_3 production, was observed in some cases in subtropical air masses (28 February 2004 and 18 February 2005), with O_3 and CO mixing ratios reaching up to 50 and 140 nmol mol^{-1}, respectively (Fig. 18a). However, in the low-level tropical air mass on 7 March 2004 a negative correlation was observed in the BL, indicating O_3 destruction, probably due to the high humidity. Air masses from the UTLS region were encountered on 28 February 2004, characterised by elevated O_3 (80–100 nmol mol^{-1}) and low CO mixing ratios (40–50 nmol mol^{-1}), and a negative correlation (Fig. 18a).

In the MCS outflow on 7 March 2004, both CO and O_3 mixing ratios were distinctly enhanced up to 140 and 90 nmol mol^{-1}, respectively, as shown in Fig. 18a. However, no distinct positive correlation was observed. Instead, the O_3 mixing ratio was rather constant for CO mixing ratios above 90 nmol mol^{-1}. The elevated O_3 mixing ratios suggest that photochemical O_3 production has taken place. However, because of the missing correlation with CO (above 90 nmol mol^{-1}) we conceive that the main ozone precursors were not from anthropogenic or biomass burning sources. Instead, LNO_x may have enhanced the rate of produced O_3, which is a source not correlated with CO. For CO mixing ratios below 90 nmol mol^{-1}, the data in Fig. 18a scatter along a mixing line between the MCS outflow data points and the air mass from the UTLS region, indicating mixing between these air masses. In addition, elevated O_3 and low CO mixing ratios along the flight track on 7 March 2004 in Fig. 6b ($\sim$47 000 s) indicate that air masses from the UTLS region were penetrated just ahead of the MCS outflow to the north.

Therefore, the origin of the elevated O_3 observed in the vicinity of the MCS outflow was probably threefold: 1) very deep convection in the MCS probably penetrated into the UTLS region and entrained O_3-rich air masses, 2) polluted air masses from the BL with elevated CO (and further ozone precursors), as discussed in Sect. 3.3.2, were ingested by the MCS, causing suitable conditions for O_3 formation, and 3) LNO_x increased the rate of produced O_3. It was however not possible to exactly determine the contribution of photochemically produced O_3 versus UTLS O_3, since no measurements are available in the BL source region to our knowledge. Measurements ahead of the MCS in the BL, along 21–22° S, indicate that O_3 was low with 20 to 30 nmol mol^{-1}, whereas O_3 measured in the aged MCS outflow exceeds 50 nmol mol^{-1}. In both cases, similar CO mixing ratios of up to 140 nmol mol^{-1} were observed, but it is not clear how representative these BL-measurements, ahead of the MCS, are in comparison to the BL around the MCS at 30° S. The correlations in Fig. 18a indicate that photochemical production was probably very efficient and enhanced O_3 to 60–70 nmol mol^{-1}. In addition, mixing with UTLS air masses, as indicated in the correlation plot, enhanced O_3 further to 70–90 nmol mol^{-1}.

Both the air mass originating from the Pacific and from the Amazon basin contained little NO_y (<0.7 nmol mol^{-1}), see Fig. 18b–c. Within the active thunderstorm system of 18 February 2005, elevated NO_y mixing ratios up to 8 nmol mol^{-1} were observed several times, as discussed in Sect. 3.3.4. The elevated NO_y was not correlated with CO, indicating that the NO_y likely originated from lightning (Fig. 18b). A slightly positive NO_y-CO correlation was observed during a descent/ascent in the polluted BL on 7 March 2004. In the MCS outflow on the same day, labelled as MCS in Fig. 18b, a slightly positive (negative) NO_y-CO correlation at the lower (upper) boundary of the yellow dots was observed, indicating the mixture of a polluted air mass (positive correlation) with an air mass from the UTLS region (negative correlation). For similar CO mixing ratios (>90 nmol mol^{-1}), NO_y mixing ratios (2–3 nmol mol^{-1}) were higher in the MCS outflow than observed ahead of the MCS in the BL (1–1.5 nmol mol^{-1}), which may partly be attributed to LNO_x.

Finally, the last correlation in Fig. 18c indicates that both O_3 and NO_y were especially elevated in the MCS outflow, compared to other air masses penetrated by the Falcon aircraft. Due to the wide horizontal ($\sim$400 km in north-south direction) and vertical ($\sim$2 km) extension of the MCS outflow, as observed by the Falcon aircraft, it is clear that these systems have a large impact on the upper tropospheric trace gas composition over Brazil.

6 Summary and conclusions

During the TROCCINOX field experiments in Brazil, in the wet seasons of 2004 and 2005, NO, NO_y, CO and O_3 mixing ratios and meteorological parameters were measured in and around thunderstorms in great detail with the DLR Falcon aircraft. This paper present results from four operation days with successful thunderstorm penetrations. A generalisation of the results is restricted due to the small number of cases studied.

Backward simulations with the FLEXPART model were partly used to determine the origin of the encountered air

masses, i.e. subtropical air masses mainly originating from the Pacific Ocean and tropical air masses originating from the Amazon basin. In both types of air masses, O_3 mixing ratios were low, between 20 and 40 nmol mol^{-1}. In the subtropical air masses, CO mixing ratios were in addition low, between 40 and 60 nmol mol^{-1}, and positively correlated with O_3. In the tropical air masses, CO mixing ratios were enhanced, between 80 and 110 nmol mol^{-1}, and negatively correlated with O_3, indicating O_3 loss processes (Jacob and Wofsy, 1990). In vicinity of thunderstorms the determination of the air mass origin with FLEXPART is not always reliable due to the small extension of many of the systems and the low background wind velocities, especially in tropical air masses. However, if the extension of the convective system is large enough (as in the MCS case presented here) and wind velocities in the UT are pronounced (as in vicinity of the subtropical jet stream), it should be resolved in the ECMWF data and therefore accounted for by FLEXPART.

Depending on the position of the South Atlantic convergence zone (SACZ), different types of thunderstorms developed in the TROCCINOX area. On the majority of the days, the SACZ was located to the north and east, and very few subtropical thunderstorms developed in the vicinity of the subtropical jet. Deep convection of tropical type developed only on a few days during the TROCCINOX field phase in the observation area (e.g. 4–5 February 2005). The SACZ was then located right over the area or to the south. In these tropical air masses, particularly narrow (~20–40 km), tall and short-lived thunderstorms with an especially low cloud base developed. The Θ_e temperatures at 850 and 500 hPa were elevated in these tropical air masses with $\geq$345 K and $\geq$332 K, respectively. In addition, the horizontal wind velocity in the UT was especially low (5–10 m s^{-1}) and no increase with altitude was observed throughout the troposphere, due to the presence of the Bolivian High. It was found, that CO mixing ratios were elevated throughout the troposphere in tropical air masses (>70 nmol mol^{-1}), due to widespread deep convection and efficient vertical mixing.

Several times during the observation period, large, persistent mesoscale convective systems (MCSs) developed over northern Argentina, Uruguay and Paraguay. The aged anvil outflow from these MCSs was occasionally advected into the TROCCINOX area. For the first time in the wet season, detailed airborne measurements in the outflow of one of these MCS succeeded, which are know to have the highest flash rates globally (Cecil et al., 2005). On 7 March 2004, distinctly enhanced NO_x, CO and O_3 mixing ratios in the range of 0.6–1.1, 110–140 and 60–70 nmol mol^{-1}, respectively, were observed in the aged outflow from a MCS that developed ~1 day earlier. These NO_x mixing ratios are as high as measured in the vicinity of the active thunderstorms. The MCS outflow observed by the aircraft covered a large area of about 400 km in the horizontal N-S direction and about 2 km in the vertical. However, LNO_x model forecasts and satellite observations of NO_2 indicate that the total extension in the N-S direction was about 800 km and in the E-W direction about 400 km. NO mixing ratios in the same range and even higher (~1–4 nmol mol^{-1}) have also been measured in large-scale NO plumes (partly from MCS) in the tropopause region over and downwind of the United States and Canada during past campaigns, e.g. NOXAR, SONEX and STREAM, and their implication for the ozone production has occasionally been pointed out (Brunner et al., 1998; Crawford et al., 2000; Jeker et al., 2000; Lange et al., 2001; Cooper et al., 2006).

The analyses of the TROCCINOX data indicate that MCS in the wet season contribute distinctly to the upper tropospheric CO, NO_y and O_3 budget over the investigated area over Brazil, which has never been observed in such detail before. High O_3 levels were observed during TROCCINOX only in the aged outflow of such MCSs. During the CITE 3 experiment in 1989 (dry season) over the equatorial and tropical South Atlantic, Andreae et al. (1994) observed aged brownish haze plumes originating from biomass burning regions in South America with elevated O_3 and CO mixing ratios up to 90 and 210 nmol mol^{-1}, respectively. Furthermore, it has been suggested that the transport of O_3 precursors from South America, e.g. biomass burning products uplifted by deep convection and NO produced by lightning, may contribute to the tropospheric O_3 maximum observed in the tropical South Atlantic basin (Pickering et al., 1996; Thompson et al., 1996; Weller et al., 1996; Edwards et al., 2003; Jenkins and Ryu, 2004; Sauvage et al., 2006). However, for our investigated MCS case the forward trajectories indicate that the O_3-rich air mass was transported into the outer region of the Bolivian High. Our observations give no indications that the O_3-rich air mass moved out over the Atlantic and influenced the South Atlantic ozone maximum.

Furthermore, it has been suggested by e.g. Thompson et al. (2000) and Ryu and Jenkins (2005) that the so-called "Atlantic ozone paradox", which is observed in the wet season (December to February), is partly influenced by the production of O_3 precursors from lightning over South America. Here we showed that O_3 was indeed distinctly enhanced in the MCS outflow, however possibly only partly due to photocatalytic O_3 production by NO_x from lightning and from the polluted BL, and partly due to mixing with O_3-rich air masses from the UTLS region. The importance of the latter source has not been pointed out clearly in most references listed above, though Thompson et al. (2000) mentioned it as a possible source. However, this transport from the UTLS region in the vicinity of MCS has also been identified from other TROCCINOX data and model simulations (cases 1 and 8 February 2005) by Konopka et al. (2006). In addition, observations at northern midlatitudes show that stratosphere-troposphere exchange may occur in the vicinity of large MCS (Poulida et al., 1996).

Furthermore, we find that the outflow from South American MCSs may contribute considerably to the elevated CO mixing ratios observed in the vicinity of the Bolivian High, at least occasionally. Earlier studies suggested biogenic

emissions in the BL over the Amazon basin (uplifted by deep convection) and long-range transport of CO-rich air masses from Africa (caused by biomass burning emissions) as the main sources of CO in the region of the Bolivian High in the wet season (Jonquieres and Marenco, 1998; Baehr et al., 2003). Here we find that CO emissions from man-made vegetation fires (savanna and grassland fires) over northern Argentina and Paraguay, and presumably anthropogenic emissions from the area around Buenos Aires may contribute considerably.

Generally during the penetrations of TROCCINOX thunderstorms, NO_x mixing ratios were enhanced in the anvil outflow region between 8 and 12.5 km (maximum flight altitude). The mean anvil-NO_x mixing ratios varied between 0.2 and 1.6 nmol mol^{-1}. NO_x in the anvil outflow from a subtropical thunderstorm was mainly attributed to lightning-produced NO_x (>80%) with minor contribution from the boundary layer (BL). Only on a few days, as in the aged MCS outflow on 7 March 2004, the contribution from the BL was significant, likely due to emissions from biomass burning and/or anthropogenic emission from larger urban areas (e.g. Buenos Aires).

These NO_x mixing ratios in Brazilian thunderstorms can be compared to our previous observations over Central Europe (Huntrieser et al., 1998; 2002). Over both regions, average lightning-produced NO_x (LNO_x) mixing ratios during anvil penetrations at 8–12.5 km were in the range of ~1 nmol mol^{-1}. Significantly higher average anvil-NO mixing ratios in the range of 1–4 nmol mol^{-1} were found during the CRYSTAL-FACE experiment in 2002 over Florida; these values were in fact higher than observed in most previous field experiments targeting thunderstorms (Ridley et al., 2004). One explanation for these higher NO mixing ratios (corresponds to about 2–6 nmol mol^{-1} NO_x) could be that CRYSTAL-FACE anvils were penetrated at higher altitudes between 12 and 16 km, where LNO_x maximizes in the anvil outflow. The investigated tropical deep convection over Brazil on 4 February 2005 also reached altitudes up to 16 km. However, the Falcon aircraft only investigated parts of the thunderstorms extending up to 10.7 km. Therefore, the main outflow region where LNO_x maximizes vertically in the investigated tropical thunderstorms was probably not probed by the Falcon aircraft. In agreement, the mean NO_x mixing ratios measured during the penetrations of the different tropical thunderstorm cells (~0.6–1.0 nmol mol^{-1}) have the tendency to increase with altitude, with the highest mixing ratios in the upper penetration level at 10.7 km (Table 2a). In contrast, during the penetrations of the subtropical thunderstorms on 28 February 2004 and 18 February 2005, the outflow altitude where LNO_x maximizes was very likely probed. According to Table 2a, the highest NO_x mixing ratios where in both cases observed in the mid penetration level (10.1 km). The repeated penetration of the latter thunderstorm (dissipating stage), indicate decreasing NO_x mixing ratios further downwind in the outflow. In this case, the measurements where performed further downwind from the lightning centre (~10–60 km), which might explain the overall lower NO_x mixing ratios (~0.2–0.8 nmol mol^{-1}), due to increased mixing with ambient air. The highest mean NO_x mixing ratios (~1.0–1.6 nmol mol^{-1}) were measured in the subtropical thunderstorm on 28 February 2004 (mature stage), where the region and altitude where LNO_x maximizes in the anvil outflow was most likely probed. However, the amount of LNO_x measured in the anvil outflow does not only depend on the position where and when the anvil was probed. Also, the number and type of lightning flashes affect the amount of LNO_x produced in the thunderstorm, which will be discussed in more detail in a forthcoming paper (Huntrieser et al., 2007[1]).

Acknowledgements. TROCCINOX was partially funded by the Commission of the European Community under the contract EVK2-CT-2001-00122. Further funding was provided by the DLR and the other TROCCINOX partners. TROCCINOX was performed as a coordinated action of European and Brazilian research institutes and agencies together with the Brazilian project TroCCiBras. We thank our Brazilian partners for their tremendous efforts to help us to make these measurements in Brazil possible, for the support during the field experiments and for providing the necessary infrastructure, in particular we thank G. Held, R. Calheiros and the team of the Instituto de Pesquisas Meterologicas (IPMET)/Universidade Estadual Paulista (UNESP) for the cooperation, which was absolutely essential for this project. We thank the company EMBRAER for hosting the team at the airport at Gaviao Peixoto in Aracatuba. We thank all the organisations, which help and support was absolutely crucial to perform the experiments in Brazil and to provide the permissions required by Brazilian law, in particular the Conseilho Nacional de Pesqisas (CNPq), the Ministerio de Ciências e Tecnologia, and the Ministerio da Defesa. We are especially grateful to A. Minikin for the excellent flight planning and his work as mission scientist on some of the flights, and to P. Stock (DLR-Oberpfaffenhofen) for instrument preparation and operation during the field campaign. We thank the pilots (M. Grossrubatscher, D. Günther, M. Hinterwaldner, and R. Welser), engineers and scientists (V. Dreiling, A. Giez, and M. Zöger) of the flight department of DLR for the excellent support during the campaigns and the preparation of the flight track maps. ECMWF and the German Weather Service are acknowledged for permitting access to the ECMWF archives. We are grateful to the ECHAM5 (MPI-Meteorology, Hamburg) and MESSy development teams (MPI-Chemistry, Mainz) for providing the preliminary version of the ECHAM5/MESSy model which was used for the forecasts in this study, and to the MATCH-MPIC forecast team for the forecast support during the field campaign. Furthermore, we thank the MODIS Rapid Response System team at NASA/GSFC and the University of Maryland (Web Fire Mapper) for the access to the MODIS fire maps, and the NCAR MOPITT team for the access to the MOPITT CO images. We express our gratitude to the lightning team at MSFC-NASA for the access to the LIS images. Finally, we are especially grateful to the two anonymous reviewers for their helpful comments, and to E. Defer (LERMA, Observatoire de Paris) and K. Pickering (NASA Goddard Space Flight Center Greenbelt) who critically reviewed draft manuscripts and gave insightful comments.

Edited by: M. G. Lawrence

References

Andreae, M. O., Anderson, B. E., Blake, D. R., Bradshaw, J. D., Collins, J. E., Gregory, G. L., Sachse, G. W., and Shipham, M. C.: Influence of plumes from biomass burning on atmospheric chemistry over the equatorial and tropical South Atlantic during CITE 3, J. Geophys. Res., 99, 12 793–12 808, 1994.

Baehr, J., Schlager, H., Ziereis, H., Stock, P., van Velthoven, P., Busen, R., Ström, J., and Schumann, U.: Aircraft observations of NO, NO_y, CO, and O_3 in the upper troposphere from 60° N to 60° S – Interhemispheric differences at midlatitudes, Geophys. Res. Lett., 30, 1598, doi:10.1029/2003GL016935, 2003.

Beirle, S., Spichtinger, N., Stohl, A., Cummins, K. L., Turner, T., Boccippio, D., Cooper, O. R., Wenig, M., Grzegorski, M., Platt, U., and Wagner T.: Estimating the NO_x produced by lightning from GOME and NLDN data: a case study in the Gulf of Mexico, Atmos. Chem. Phys., 6, 1075–1089, 2006, http://www.atmos-chem-phys.net/6/1075/2006/.

Boccippio, D. J., Koshak, W. J., and Blakeslee, R. J.: Performance assessment of the tropical transient detector and lightning imaging sensor. Part I: Predicted diurnal variability, J. Atmos. Oceanic Technol., 19, 1318–1332, 2002.

Bolton, D.: The computation of equivalent potential temperature, Mon. Wea. Rev., 108, 1046–1053, 1980.

Bond, D. W., Steiger, S., Zhang, R., Tie, X., and Orville, R. E.: The importance of NO_x production by lightning in the tropics, Atmos. Environ., 36, 1509–1519, 2002.

Bowensmann, H., Burrows, J. P., Buchwitz, M., Frerick, J., Rozanov, V. V., Chance, K. V., and Goede, A. P. H.: SCIAMACHY: Mission objectives and measurement modes, J. Atmos. Sci., 56, 127–150, 1999.

Brooks, H. E., Lee, J. W., and Craven, J. P.: The spatial distribution of severe thunderstorm and tornado environments from global reanalysis data, Atmos. Environ., 67–68, 73–94, 2003.

Brunner, D., Staehelin, J., and Jeker, D.: Large-scale nitrogen oxide plumes in the tropopause region and implications for ozone, Science, 282, 1305–1309, 1998.

Burrows, J. P., Hölzle, E., Goede, A. P. H., Visser, H., and Fricke, W.: SCIAMACHY- Scanning Imaging Absorption Spectrometer for Atmospheric Chartography, Acta Astronautica, 35, 7, 445–451, 1995.

Carvalho, L. M. V., Jones, C., and Silva Dias, M. A. F.: Intraseasonal large-scale circulations and mesoscale convective activity in tropical South America during the TRMM-LBA campaign, J. Geophys. Res., 107, doi:10.1029/2001JD000745, LBA 9-1–LBA 9-20, 2002.

Carvalho, L. M. V., Jones, C., and Liebmann, B.: The South Atlantic convergence zone: Intensity, form, persistence and relationships with intraseasonal to interannual activity and extreme rainfall, J. Climate, 17, 88–108, 2004.

Cecil, D. J., Goodman, S. J., Boccippio, D. J., Zipser, E. J., and Nesbitt, S. W.: Three years of TRMM precipitation features. Part I: Radar, radiometric, and lightning characteristics, Mon. Wea. Rev., 133, 543–566, 2005.

Chaboureau, J.-P., Cammas, J.-P., Duron, J., Mascart, P. J., Sitnikov, N., and Voessing, H.-J.: A numerical study of tropical cross-tropopause transport by convective overshoots, Atmos. Chem. Phys., 7,1731–1740, 2007.

Chameides, W. L. and Walker, J. C. G.: A photochemical theory of tropospheric ozone, J. Geophys. Res., 78, 8751–8760, 1973.

Christian, H. J., Blakeslee, R. J., Goodman, S. J., et al.: The Lightning Imaging Sensor, Proceedings of the 11th International Conference on Atmospheric Electricity, Guntersville, Alabama, 7–11 June 1999, pp. 746–749, 1999.

Christian, H. J., Blakeslee, R. J., Boccippio, D. J., et al.: Global frequency and distribution of lightning as observed from space by the Optical Transient Detector, J. Geophys. Res., 108, 4005, doi:10.1029/2002JD002347, 2003.

Cooper, O. R., Stohl, A., Trainer, M., et al.: Large upper tropospheric ozone enhancements above mid-latitude North America during summer: In situ evidence from the IONS and MOZAIC ozone measurement network, J. Geophys. Res., 111, D24S05, doi:10.1029/2006JD007306, 2006.

Crawford, J., Davis, D., Olson, J., et al.: Evolution and chemical consequences of lightning-produced NO_x observed in the North Atlantic upper troposphere, J. Geophys. Res., 105, 19 795–19 809, 2000.

Crutzen, P. J.: The influence of nitrogen oxides on the atmospheric ozone content, Q. J. Roy. Meteor. Soc., 96, 320–327, 1970.

Davies, D., Kumar, S., and Descloitres, J.: Global fire monitoring using MODIS near-real-time satellite data, GIM International, 18(4), 41–43, 2004.

Dickerson, R. R.: Measurements of reactive nitrogen compounds in the free troposphere, Atmos. Environ., 18, 2585–2593, 1984.

Drummond, J. R. and Mand, G. S.: The Measurements of Pollution in the Troposphere (MOPITT) Instrument: Overall Performance and Calibration Requirements, J. Atmos. Ocean. Tech., 13, 314–320, 1996.

Dye, J. E., Ridley, B. A., Skamarock, W., et al.: An overview of the Stratospheric-Tropospheric Experiment: Radiation, aerosols, and ozone (STERAO)-Deep convection experiment with results for the July 10, 1996 storm, J. Geophys. Res., 105, 10 023–10 045, 2000.

Edwards, D. P., Halvorson, C. M., and Gille, J. C.: Radiative transfer modeling for the EOS Terra satellite Measurement of Pollution in the Troposphere (MOPITT) instrument, J. Geophys. Res., 104, 16 755–16 775, 1999.

Edwards, D. P., Lamarque, J.-F., Attié, J.-L. et al.: Tropospheric ozone over the tropical Atlantic : A satellite perspective, J. Geophys. Res., 108, 4237, doi:10.1029/2002JD002927, 2003.

Emanuel, K. A. and Živcovizc'-Rothman, M.: Development and evaluation of a convection scheme for use in climate models, J. Atmos. Sci., 56, 1766–1782, 1999.

Folkins, I., Oltmans, S. J., and Thompson, A. M.: Tropical convective outflow and near surface equivalent potential temperature, Geophys. Res. Lett., 27, 2549–2552, 2000.

Forster, C., Stohl, A., and Seibert, P.: Parameterization of convective transport in a Lagrangian particle dispersion model and its evaluation, J. Appl. Meteor. Clim., 46, 403-422, 2007.

Gatti, L. V., Cordova, A. M., Yamazaki, A., et al.: Trace gas measurements in the Amazon basin during the wet and dry season, in: A changing atmosphere, Proc. of 8th European Symposium on the Physico-Chemical Behaviour of Atmospheric Pollutants, 17–20 Sept., Torino, Italy, edited by: J. Hjorth and F. Raes, 2001.

Gerbig, C., Schmitgen, S., Kley, D., Volz-Thomas, A., Dewey, K.,

and Haaks, D.: An improved fast-response vacuum-UV resonance fluorescence CO instrument, J. Geophys. Res., 104, 1699–1704, 1999.

Giglio, L., Descloitres, J., Justice, C. O., and Kaufman, Y. J.: An enhanced contextual fire detection algorithm for MODIS, Rem. Sens. Environ., 87, 273–282, 2003.

Grewe, V., Brunner, D., Dameris, M., Grenfell, J. L., Hein, R., Shindell, D., and Staehelin, J.: Origin and variability of upper tropospheric nitrogen oxides and ozone at northern mid-latitudes, Atmos. Environ., 35, 3421–3433, 2001.

Harriss, R. C., Sachse, G. W., Hill, G. F., Wade, L. O., and Gregory, G. L.: Carbon monoxide over the Amazon Basin during the wet season, J. Geophys. Res., 95, 16 927–16 932, 1990.

Hauglustaine, D., Emmons, L., Newchurch, M., et al.: On the role of lightning NO_x in the formation of tropospheric ozone plumes: A global model perspective, J. Atmos. Chem., 38, 277–294, 2001.

Highwood, E. J. and Hoskins, B. J.: The tropical tropopause, Q. J. R. Meteorol. Soc., 124, 1579–1604, 1998.

Hild, L., Richter, A., Rozanov, V., and Burrows, J. P.: Air Mass Calculations for GOME Measurements of lightning-produced NO_2, Adv. Space Res., 29(11), 1685–1690, 2002.

Höller, H., Finke, U., Huntrieser, H., Hagen, M., and Feigl, C.: Lightning produced NO_x (LINOX) - Experimental design and case study results, J. Geophys. Res., 104, 13 911–13 922, 1999.

Houze, R. A.: Cloud Dynamics, Academic, San Diego, California, 573 pp., 1993.

Houze, R. A.: Mesoscale convective systems, Rev. Geophys., 42, RG4003, doi:2004RG000150, 2004.

Huntrieser, H., Schlager, H., Feigl, C., and Höller, H.: Transport and production of NO_x in electrified thunderstorms: Survey of previous studies and new observations at midlatitudes, J. Geophys. Res., 103, 28 247–28 264, 1998.

Huntrieser, H., Feigl, C., Schlager, H., Schröder, F., Gerbig, C., van Velthoven, P., Flatøy, F., Théry, C., Petzold, A., Höller, H., and Schumann, U.: Airborne measurements of NO_x, tracer species and small particles during the European Lightning Nitrogen Oxides Experiment, J. Geophys. Res., 107(D11), 4113, doi: 10.1029/2000JD000209, 2002.

Huntrieser, H., Heland, J., Schlager, H., et al.: Intercontinental air pollution transport from North America to Europe: Experimental evidence from airborne measurements and surface observations, J. Geophys. Res., 110, D01305, doi:10.1029/2004JD005045, 2005.

Jacob, D. J. and Wofsy, S. C.: Budgets of reactive nitrogen, hydrocarbons, and ozone over the Amazon forest during the wet season, J. Geophys. Res., 95, 16 737–16 754, 1990.

Jacob, D. J., Heikes, B. G., Fan, S.-M., et al.: Origin of ozone and NO_x in the tropical troposphere : A photochemical analysis of aircraft observations over the South Atlantic basin, J. Geophys. Res., 101, 24 235–24 250, 1996.

Jaeglé, L., Jacob, D. J., Brune, W. H., et al.: Ozone production in the upper troposphere and the influence of aircraft during SONEX: Approach of NO_x-saturated conditions, Geophys. Res. Lett., 26, 3081–3084, 1999.

Jeker, D., Pfister, L., Thompson, A. M., Brunner, D., Boccippio, D. J., Pickering, K. E., Wernli, H., Kondo Y., and Staehelin, J.: Measurement of nitrogen oxides at the tropopause: Attribution to convection and correlation with lightning, J. Geophys. Res., 105, 3679–3700, 2000.

Jenkins, G. S. and Rye, J.-H.: Space-borne observations link the tropical Atlantic ozone maximum and paradox to lightning, Atmos. Chem. Phys., 4, 361–375, 2004, http://www.atmos-chem-phys.net/4/361/2004/.

Jeuken, A. B. M., Siegmund, P. C., Heijboer, L. C., Feichter, J., and Bengtsson, L.: On the potential of assimilating meteorological analyses in a global climate model for the purpose of model validation, J. Geophys. Res., 101, 16 939–16 950, 1998.

Jöckel, P., Sander, R., Kerkweg, A., Tost, H., and Lelieveld, J.: Technical Note: The Modular Earth Submodel System (MESSy) – a new approach towards Earth System Modeling, Atmos. Chem. Phys., 5, 433–444, 2005, http://www.atmos-chem-phys.net/5/433/2005/.

Jöckel, P., Tost, H., Pozzer, A., et al.: The atmospheric chemistry general circulation model ECHAM5/MESSy1: Consistent simulation of ozone from the surface to the mesosphere, Atmos. Chem. Phys., 6, 5067–5104, 2006, http://www.atmos-chem-phys.net/6/5067/2006/.

Jonquieres, I. and Marenco, A.: Distribution by deep convection and long-range transport of CO and CH_4 emissions from the Amazon basin, as observed by the airborne campaign TROPOZ II during the wet season, J. Geophys. Res., 103, 19 075–19 091, 1998.

Justice, C. O., Giglio, L., Korontzi, S., Owens, J., Morisette, J. T., Roy, D., Descloitres, J., Alleaume, S., Petitcolin, F., and Kaufman, Y. J.: The MODIS fire products, Rem. Sens. Environ., 83, 244–262, 2002.

Kodama, Y. M.: Large-scale common features of subtropical precipitation zones (the Baiu frontal zone, the SPCZ, and the SACZ). Part I: Characteristics of subtropical frontal zones, J. Meteor. Soc. Japan, 70, 813–835, 1992.

Kodama, Y. M.: Large-scale common features of subtropical convergence zones (the Baiu frontal zone, the SPCZ, and the SACZ). Part II: Conditions of the circulations for generating STCZs, J. Meteor. Soc. Japan, 71, 581–610, 1993.

Konopka, P., Günther, G., Müller, R., et al.: Contribution of mixing to the upward transport across the TTL, Atmos. Chem. Phys. Discuss., 6, 12 217–12 266, 2006.

Kurz, C.: Entwicklung und Anwendung eines gekoppelten Klima-Chemie-Modellsystems, PhD Thesis, Ludwig-Maximilians-Universität München, http://edoc.ub.uni-muenchen.de/archive/00004804/01/Kurz_Christian.pdf, , 142 pp., 2006.

Laing, A. G. and Fritsch, J. M.: The global population of mesoscale convective complexes, Q. J. Roy. Meteor. Soc., 123, 389–405, 1997.

Lamarque, J.-F., Brasseur, G. P., Hess, P. G., and Müller, J.-F.: Three-dimensional study of the relative contributions of the different nitrogen sources in the troposphere, J. Geophys. Res., 101, 22 955–22 968, 1996.

Lange, L., Hoor, P., Helas, G., et al.: Detection of lightning-produced NO in the midlatitude upper troposphere during STREAM 1998, J. Geophys. Res., 106, 27 777–27 785, 2001.

Levy II, H., Moxim, W. J., and Kasibhatla, P. S.: A global three-dimensional time-dependent lightning source of tropospheric NO_x, J. Geophys. Res., 101, 22 911–22 922, 1996.

Levy II, H., Moxim, W. J., Klonecki, A. A., and Kasibhatla, P. S.: Simulated tropospheric NO_x: Its evaluation, global distribution and individual source contributions, J. Geophys. Res., 104,

26 279–26 306, 1999.

Luke, W. T., Dickerson, R. R., Ryan, W. F., Pickering, K. E., and Nunnermacker, L. J.: Tropospheric chemistry over the lower Great Plains of the United States, 2, Trace gas profiles and distributions, J. Geophys. Res., 97, 20 647–20 670, 1992.

Machado, L. A. T., Russow, W. B., Guedes, R. L., and Walker, A. W.: Life cycle variations of mesoscale convective systems over the Americas, Mon. Wea. Rev., 126, 1630–1654, 1998.

Maddox, R. A.: An objective technique for separating macroscale and mesoscale features in meteorological data, Mon. Wea. Rev., 108, 1108–1121, 1980.

Mari, C., Chaboureau, J. P., Pinty, J. P., et al.: Regional lightning NO_x sources during the TROCCINOX experiment, Atmos. Chem. Phys., 6, 5559–5572, 2006, http://www.atmos-chem-phys.net/6/5559/2006/.

Martin, R. V., Jacob, D. J., Logan, J. A., Ziemke, J. M., and Washington R.: Detection of a lightning influence on tropical tropospheric ozone, Geophys. Res. Lett., 27, 1639–1642, 2000.

Meyer, C. P., Elsworth, C. M., and Galbally, I. E.: Water vapour interference in the measurement of ozone in ambient air by ultraviolet absorption, Rev. Sci. Instrum., 62, 223–228, 1991.

Mushtak, V. C., Williams, E. R., and Boccippio, D. J.: Latitudinal variations of cloud base height and lightning parameters in the tropics, Atmos. Res., 76, 222–230, 2005.

Nesbitt, S. W., Zipser, E. J., and Cecil, D. J.: A census of precipitation features in the tropics using TRMM: Radar, ice scattering, and lightning observations, J. Climate, 13, 4087–4106, 2000.

Petersen, W. A., Nesbitt, S. W., Blakeslee, R. J., Hein, P., Cifelli, R., and Rutledge, S. A.: TRMM observations of intraseasonal variability in convective regimes over the Amazon, J. Climate, 15, 1278–1294, 2002.

Pickering, K. E., Thompson, A. M., Tao, W.-K., and Kucsera, T. L.: Upper tropospheric ozone production following mesoscale convection during STEP/EMEX, J. Geophys. Res., 98, 8737–8749, 1993.

Pickering, K. E., Thompson, A. M., Wang Y., et al.: Convective transport of biomass burning emissions over Brazil during TRACE A, J. Geophys. Res., 101, 23 993–24 012, 1996.

Pickering, K. E., Wang, Y., Tao, W. K., Price, C., and Müller, J. F.: Vertical distribution of lightning NO_x for use in regional and global chemical transport models, J. Geophys. Res., 103, 31 203–31 216, 1998.

Pinto, I. R. C. A. and Pinto Jr., O.: Cloud-to-ground lightning distributions in Brazil, J. Atmos. Sol.-Terr. Phys., 65, 733–737, 2003.

Poulida, O., Dickerson, R. R., and Heymsfield, A. : Stratosphere-troposphere exchange in a midlatitude mesoscale convective complex, 1, Observations, J. Geophys. Res., 101, 6823–6936, 1996.

Price, C. and Rind, D.: What determines the cloud-to-ground lightning fraction in thunderstorms?, Geophys. Res. Lett., 20, 463–466, 1993.

Richter, A., Burrows, J. P., Nüß, H., Granier, C., and Niemeier, U.: Increase in tropospheric nitrogen dioxide over China observed from space, Nature, 437, 129–132, doi:10.1038/nature04092, 2005.

Ridley, B. A., Walega, J. G., Dye, J. E., and Grahek, F. E.: Distributions of NO, NO_x, NO_y, and O_3 to 12 km altitude during the summer monsoon season over New Mexico, J. Geophys. Res., 99, 25 519–25 534, 1994.

Ridley, B. A., Dye, J. E., Walega, J. G., Zheng, J., Grahek, F. E., and Rison, W.: On the production of active nitrogen by thunderstorms over New Mexico, J. Geophys. Res., 101, 20 985–21 005, 1996.

Ridley, B. A., Ott, L., Pickering, K., et al.: Florida thunderstorms: A faucet of reactive nitrogen to the upper troposphere, J. Geophys. Res., 109, D17305, doi:10.1029/2004JD004769, 2004.

Ridley, B. A., Avery, M. A., Plant, J. V., Vay, S. A., Montzka, D. D., Weinheimer, A. J., Knapp, D. J., Dye, J. E., and Richard, E. C.: Sampling of chemical constituents in electrically active convective systems: Results and cautions, J. Atmos. Chem., 54, 1–20, 2006.

Roeckner, E., Brokopf, R., Esch, M., Giorgetta, M., Hagemann, S., Kornblueh, L., Manzini, E., Schlese, U., and Schulzweida, U.: Sensitivity of simulated climate to horizontal and vertical resolution in the ECHAM5 atmosphere model, J. Climate, 19, 3771–3791, 2006.

Ryu, J.-H. and Jenkins, G. S.: Lightning-tropospheric ozone connections: EOF analysis of TCO and lightning data, Atmos. Environ., 39, 5799–5805, 2005.

Saba, M. M. F., Ballarotti, M. G., and Pinto Jr., O.: Negative cloud-to-ground lightning properties from high-speed video observations, J. Geophys. Res., 111, D03101, doi:10.1029/2005JD006415, 2006.

Salio, P., Nicolini, M., and Zipser E. J.: Mesoscale convective systems over southeastern South America and their relationship with the South American low-level jet, Mon. Wea. Rev., 135, 1290–1309, 2007.

Sander, R., Kerkweg, A., Jöckel, P., and Lelieveld, J.: Technical note: The new comprehensive atmospheric chemistry module MECCA, Atmos. Chem. Phys., 5, 445–450, 2005, http://www.atmos-chem-phys.net/5/445/2005/.

Sato, M., and Fukunishi, H: Global sprite occurrence locations and rates derived from triangulation of transient Schumann resonance events, Geophys. Res. Lett., 30, 1859, doi:10.1029/2003GL017291, 2003.

Satyamurty, P., Nobre, C., and Silva Dias, P. L.: South America. Meteorology of the Southern Hemisphere, D. J. Karoly and D. G. Vincent, Eds., Amer. Meteor. Soc., 119–139, 1998.

Sauvage, B., Martin, R. V., van Donkelaar, A., Liu, X., Chance, K., Jaeglé, L., Palmer, P. I., Wu, S., and Fu, T.-M.: Remote sensed and in situ constraints on processes affecting tropical tropospheric ozone, Atmos. Chem. Phys., 7, 815–838, 2007, http://www.atmos-chem-phys.net/7/815/2007/.

Sauvage, B., Thouret, V., Thompson, A. M., Witte, J. C., Cammas, J.-P., Nédélec, P., and Athier, G.: Enhanced view of the "tropical Atlantic ozone paradox" and "zonal wave one" from the in situ MOZAIC and SHADOZ data, J. Geophys. Res., 111, D01301, doi:10.1029/2005JD006241, 2006.

Schlager, H., Konopka, P., Schulte, P., Schumann, U., Ziereis, H., Arnold, F., Klemm, M., Hagen, D. E., Whitefield, P. D., and Ovarlez, J.: In situ observations of air traffic emission signatures in the North Atlantic flight corridor, J. Geophys. Res., 102, 10 739–10 750, 1997.

Schultz, M. G., Jacob, D. J., Wang, Y., et al.: On the origin of tropospheric ozone and NO_x over the tropical South Pacific, J. Geophys. Res., 104, 5829–5843, 1999.

Schumann, U., Konopka, P., Baumann, R., Busen, R., Gerz, T., Schlager, H., Schulte P., and Volkert, H.: Estimate of diffusion

parameters of aircraft exhaust plumes near the tropopause from nitric oxide and turbulence measurements, J. Geophys. Res., 100, 14 147–14 162, 1995.

Schumann, U., Huntrieser, H., Schlager, H., Bugliaro, L., Gatzen, C., and Hoeller, H.: Nitrogen Oxides from thunderstorms – Results from experiments over Europe and the Continental Tropics, paper presented at Deutsch-Österreichisch-Schweizerische Meteorologen-Tagung (DACH), Deutsche Meteorologische Gesellschaft, Karlsruhe, Germany, 7–10 September, 2004.

Schumann, U. and Huntrieser, H.: The global lightning–induced nitrogen oxides source, Atmos. Chem. Phys. Discuss., 7, 2623–2818, 2007, http://www.atmos-chem-phys-discuss.net/7/2623/2007/.

Seibert, P. and Frank, A.: Source-receptor matrix calculation with a Lagrangian particle dispersion model in backward mode, Atmos. Chem. Phys., 4, 51–63, 2004, http://www.atmos-chem-phys.net/4/51/2004/.

Siqueira, J. R., Rossow, W. B., Machado, L. A. T., and Pearl, C.: Structural characteristics of convective systems over South America related to cold-frontal incursions, Mon. Wea. Rev., 133, 1045–1064, 2005.

Smyth, S. B., Sandholm, S. T., Bradshaw, J. D., et al.: Factors influencing the upper free tropospheric distribution of reactive nitrogen over the South Atlantic during the TRACE A experiment, J. Geophys. Res., 101, 24 165–24 186, 1996.

Stith, J., Dye, J., Ridley, B., Laroche, P., Defer, E., Baumann, K., Hübler, G., Zerr, R., and Venticinque, M.: NO signatures from lightning flashes, J. Geophys. Res., 104, 16 081–16 089, 1999.

Stohl, A., Hittenberger, M., and Wotawa, G.: Validation of the Lagrangian particle dispersion model FLEXPART against large scale tracer experiment data, Atmos. Environ., 32, 4245–4264, 1998.

Stohl, A., Forster, C., Eckhardt, S., Huntrieser, H., Heland, J., Schlager, H., Aufmhoff, H., Arnold, F., and Cooper, O.: A backward modeling study of intercontinental pollution transport using aircraft measurements, J. Geophys. Res., 108, 4370, doi:10.1029/2002JD002862, 2003.

Stohl, A., Forster, C., Frank, A., Seibert, P., and Wotawa, G.: Technical Note: The Lagrangian Particle Dispersion Model FLEXPART Version 6.2, Atmos. Chem. Phys., 5, 2461–2474, 2005, http://www.atmos-chem-phys.net/5/2461/2005/.

Strand, A. and Hov, Ø.: The impact of man-made and natural NO_x emissions on upper tropospheric ozone: A two-dimensional model study, Atmos. Environ., 30, 1291–1303, 1996.

Thomas, J. N., Taylor, M. J., Pautet, D., et al.: A very active sprite-producing storm observed over Argentina, EOS, Transactions, AGU, 88, 10, 117–119, 2007.

Thomas, R. J., Krehbiel, P. R., Rison, W., Hamlin, T., Boccippio, D. J., Goodman, S. J., and Christian, H. J.: Comparison of ground-based 3–dimensional lightning mapping observations with satellite-based LIS observations in Oklahoma, Geophys. Res. Lett., 27, 1703–1706, 2000.

Thompson, A. M., Pickering, K. E., McNamara, D. P., Schoeberl, M. R., Hudson, R. D., Kim, J. H., Browell, E. V., Kirchhoff, V. W. J. H., and Nganga, D.: Where did tropical ozone over southern Africa and the tropical Atlantic come from in October 1992? Insights from TOMS, GTE TRACE A, and SAFARI 1992, J. Geophys. Res., 101, 24 251–24 278, 1996.

Thompson, A. M., Doddridge, B. G., Witte, J. C., Hudson, R. D., Luke, W. T., Johnson, J. E., Johnson, B. J., Oltmans, S. J., and Weller, R.: A tropical Atlantic paradox: Shipboard and satellite views of a tropospheric ozone maximum and wave-one in January–February 1999, Geophys. Res. Lett., 27, 3317–3320, 2000.

Torres, A. L. and Buchan, H.: Tropospheric nitric oxide measurements over the Amazon Basin, J. Geophys. Res., 93, 1396–1406, 1988.

Velasco, I. and Fritsch, J. M.: Mesoscale convective complexes in the Americas, J. Geophys. Res., 92, 9591–9613, 1987.

Volz-Thomas, A., Lerner, A., Pätz, H.-W., Schultz, M., McKenna, D. S., Schmitt, R., Madronich, S., and Röth, E. P.: Airborne measurements of the photolysis frequency of NO_2, J. Geophys. Res., 101, 18 613–18 627, 1996.

Weller, R., Lilischkis, R., Schrems, O., Neuber, R., and Wessel, S.: Vertical ozone distribution in the marine atmosphere over the central Atlantic Ocean (56° S-50° N), J. Geophys. Res., 101, 1387–1400, doi:95JD02838, 1996.

Williams, E., Rosenfeld, D., Madden, N., et al.: Contrasting convective regimes over the Amazon: Implications for cloud electrification, J. Geophys. Res., 107, 8082, doi:10.1029/2001JD000380, 2002.

Zahn, A., Brenninkmeijer, C. A. M., Crutzen, P. J., et al.: Electrical discharge source for tropospheric "ozone-rich transients", J. Geophys. Res., 107, 4638, doi:10.1029/2002JD002345, 2002.

Zipser, E. J., Cecil, D. J., Liu, C., Nesbitt, S. W., and Yorty, D. P.: Where are the most intense thunderstorms on Earth?, B. Am. Meteor. Soc., 8, 1057–1071, 2006.